PL-TR-93-2167



# EYESAFE RARE EARTH CRYSTAL LASERS FOR ATMOSPHERE SOUDINGS

Milton Birnbaum

University of Southern California
Center for Laser Studies
University Park, DRB 17
Los Angeles, CA 90089-1112

1 August 1993

Final Report
5 September 1989-31 May 1993



Approved for public release; distribution unlimited



PHILLIPS LABORATORY
Directorate of Geophysics
AIR FORCE MATERIEL COMMAND
HANSCOM AIR FORCE BASE, MA 01731-3010

"This technical report has been reviewed and is approved for publication"

(Signature)
STEVEN B. ALEJANDRO
CONTRACT MANAGER

(Signature)
DONALD E. BEDO, CHIEF
ELECTRO-OPTICAL MEASUREMENTS BR.

(Signature)
ROGER A. VAN TASSEL, IRECTOR
OPTICAL ENVIRONMENT DIVISION

This report has been reviewed by the ESC Public Affairs Office (PA) and is releasable to the National Technical Information Service (NTIS).

Qualified requestors may obtain additional copies from the Defense Technical Information Center. All others should apply to the National Technical Information Service.

If your address has changed, or if you wish to be removed from the mailing list, or if the addressee is no longer employed by your organization, please notify PL/TSI, Hanscom AFB, MA 01731-3010. This will assist us in maintaining a current mailing list.

Do not return copies of this report unless contractual obligations or notices on a specific document requires that it be returned.

# REPORT DOCUMENTATION PAGE

Form Approved
OMB No 0704-0188



| 1. AGENCY USE ONLY (Leave blank) | 2. REPORT DATE | 3. REPORT TYPE AND DATES COVERED |
|---|---|---|
| | 1 August 1993 | Final Technical Report (9/5/89 - 5/31/93) |

**4. TITLE AND SUBTITLE**
Eyesafe Rare Earth Crystal Lasers for Atmosphere Soundings

**5. FUNDING NUMBERS**
Contract No.:
F19628-89-K-0038
PE 62101F
PR 7670 TA 16 WU BA

**6. AUTHOR(S)**
Milton Birnbaum

**7. PERFORMING ORGANIZATION NAME(S) AND ADDRESS(ES)**
University of Southern California
Department of Electrical Engineering - Electrophysics
Center for Laser Studies
University Park - DRB 17
Los Angeles, CA 90089-1112

**8. PERFORMING ORGANIZATION REPORT NUMBER**

**9. SPONSORING/MONITORING AGENCY NAME(S) AND ADDRESS(ES)**
Phillips Laboratory
29 Randolph Road
Hanscom AFB, MA 01731-3010
Contract Manager: S. Alejandro/GPOA

**10. SPONSORING/MONITORING AGENCY REPORT NUMBER**
PL-TR-93-2167

**11. SUPPLEMENTARY NOTES**

**12a. DISTRIBUTION AVAILABILITY STATEMENT**
Approved for Public Release: Distribution Unlimited

**12b. DISTRIBUTION CODE**

**13. ABSTRACT (Maximum 200 words)**

**The characteristics of room temperature $Er^{3+}$:YAG lasers at 1.644μ end pumped by an $Er^{3+}$:glass laser at 1.535μ are described. Low threshold and efficient operation was obtained for 0.5 and 1% $Er^{3+}$:YAG. Similar studies were performed utilizing 0.7% $Er^{3+}$(3% $Yb^{3+}$, 1% $Cr^{3+}$) YSGG. Laser action of $Er^{3+}$:YSGG at 1.643μ was achieved for the first time.**

| 14. SUBJECT TERMS | 15. NUMBER OF PAGES |
|---|---|
| **Solid state lasers; $Er^{3+}$:YAG:1.64 microns; $Er^{3+}$:YSGG:1.64 microns** | 90 |
| | 16. PRICE CODE |

| 17. SECURITY CLASSIFICATION OF REPORT | 18. SECURITY CLASSIFICATION OF THIS PAGE | 19. SECURITY CLASSIFICATION OF ABSTRACT | 20. LIMITATION OF ABSTRACT |
|---|---|---|---|
| UNCLASSIFIED | UNCLASSIFIED | UNCLASSIFIED | SAR |

# CONTENTS

## INTRODUCTION

The focus of this research program was to establish the feasibility of the development of eye-safe lasers operating within an atmospheric window which could then find application in atmospheric sounding and wind-sat applications. Er:crystal lasers (Er:YAG at 1. 64 mm and Er:YSGG at 1.64 mm) meet the above criteria and could be utilized for these applications. During the period of this work, interest in the development of eye-safe solid state lasers in particular eye lasers operating near 1.5 mm, has intensified because of the potential applicability of Er:YAG eye-safe lasers.

## RESULTS AND ACCOMPLISHMENTS

All of the major results of our studies are in the process of publication or submission for publication. Therefore our final report consists of copies of our papers in proces of publication, accepted for publication and the draft copies of those in process of publication. One Ph.D. Thesis (Electrical Engineering) has been completed under this contract: "Dynamic of Eye-Safe (1. 6 m) Er Lasers" by Kalin Spariosu, May 1993. Copies of the following papers are given in this final report:

1. "Room-Temperature 1.644 Micron Er:YAG Lasers", K.Spariosu and M. Birnbaum, OSA Proceedings on Advanced Solid-State Lasers, 1992, Vol. 13 Lloyd L. Chase and Albert A. Pinto (eds), pp 1276-130.

2. "Intra-Cavity 1.549 m Pumped 1.634 M Er:YAG Lasers at 300K", K. Spariosu and M. Birbaum accepted for publication in IEEE Jour. of Quantum Electronics.

3. "Er:YAG Laser Dynamics: Effects of upconversion", K. Spariosu, M. Birnbaum and Bruno Viana submitted to JOSA B special issue on Upconversion Lasers.

4. "1.634 m Er:YSGG at 300 K", K. Spariosu, M. Birnbaum and M. Kokta submitted to IEEE Jour. Quantum Electronics.

## CONCLUDING RESTATEMENT OF ACCOMPLISHMENTS

The results of our investigation indicates tht Er:YAG is the crystal of choice for development of a 1.64 m eye-safe laser and that a diode-pumped version of this laser suitable for air-borne and/or satellite application can be developed. The scientific basis for the above assertions will be found in the paper included in this final report.

# INTRA-CAVITY 1.549μm PUMPED 1.634μm Er:YAG LASERS AT 300K

Kalin Spariosu and Milton Birnbaum

Center for Laser Studies

University of Southern California

University Park, DRB 17

Los Angeles, CA 90089-1112

## Abstract

A novel method of generating 1.634μm laser action from Er:YAG crystals pumped intra-cavity by an Er:glass laser emitting at 1.549μm is described. Operation of the Er:glass laser at 1.549μm ( red shifted from the standard 1.532μm, but with comparable output) at 300K was obtained using mirrors with tailored spectral reflectivities. Several Er:YAG crystals ranging in concentration from 0.3% to 2% and in length from 1cm to 8cm were lased in the intra-cavity pumping arrangement. All the Er:YAG crystals lased in the $^4I_{13/2}$: Y1(6544cm$^{-1}$)-$^4I_{15/2}$: Z6(424cm$^{-1}$) 1.634μm transition at 300K.

## Introduction

The first 1.6μm $^4I_{13/2}$-$^4I_{15/2}$ laser action was demonstrated in Er:$CaWO_4$[1] followed by reported laser action in Er:$CaF_2$[2], and in Er:$LaF_3$[3] near 1.6μm. All the above reports utilized flash lamp pumping at 77K. The first 1.645μm $^4I_{13/2}$-$^4I_{15/2}$ laser action in Er:YAG was achieved by Johnson et al[4] at 77K, and later at room temperature, White and Schleusener[5], again using flash lamp excitation in both cases. More recently, CW oscillation at 1.645μm in Er:YAG was achieved using a Kr ion laser at 0.647μm in an end pumping arrangement[6,7]. We reported 1.532μm pumped 1.645μm Er:YAG lasers at 300K using an Er:glass laser as the pump source in an end pumped configuration[8]. All of the above reported Er:YAG lasers at 300K oscillated in the $^4I_{13/2}$:Y3(6602$cm^{-1}$)-$^4I_{15/2}$:Z7(523$cm^{-1}$) transition at 1.645μm. Zverev et al[9] reported on a flash-lamp pumped 1.632±2μm $^4I_{13/2}$:Y3(6549$cm^{-1}$)-$^4I_{15/2}$:Z7(426$cm^{-1}$) Er:YAG laser action at 300K.

The first Intra-Cavity (IC) pumped laser was demonstrated by Gapontsev et al [11] where they pumped an Yb, Er:glass laser with a flash-lamp pumped 1.054μm Nd:glass laser. Their Er:glass laser output manifested itself in 3 different spectral lines: 1.536μm near threshold, 1.536μm and 1.543μm at 1.5 times above threshold, and 1.536μm, 1.543μm, 1.538μm at 2.5 times above threshold, the 1.543μm and the 1.538μm being the

weaker lines. This report was followed by a more extensive study of IC Nd:YAG pumping of Yb,Er:glass lasers in several different glass bases ( silicates to phosphates) done by Kalinin et al [12].

Further work on the IC Nd:YAG laser pumped Yb,Er:glass laser done by Murzin and Fromzel[13] yielded a theoretical predicition of the optimum pump absorption coefficient in Yb,Er:glass to be $\alpha_{1.06\mu m} \approx 0.05 cm^{-1}$. More recently, Aubakirov et al[14] demonstrated a method of raising efficiency of the IC Nd laser pumped Yb,Er:glass laser by the introduction of a spectrally limiting etalon in the cavity. This essentially prevents the shift of the 1.06μm Nd laser output toward longer wavelengths when an IC Yb,Er:glass load is introduced ( also noted by Kalinin et al[12]). A recent report of an IC 1.06μm Nd:YAG laser pumped Yb,Er:glass laser was done by Anthon and Pier[15], where they utilized diode lasers as the means of exciting the Nd:YAG laser. They noted high efficiencies but limited power scaling potential due to low thermal conductivity of the phosphate glass host. The authors did note, however, that the anticipated Nd:YAG laser wavelength shift ( due to the Yb,Er:glass IC load) did not occur and the 1.06μm pump wavelength remained unchanged.

Other reports on IC lasers included a 3μm Ho:$YAlO_3$ laser IC pumped by a flash-lamp pumped 1.079μm Nd:$YAlO_3$ laser[16], a 2.1μm Ho:YAG laser IC pumped by a flash-lamp pumped 2μm Cr,Tm:YAG laser[17], and a 2.1μm Ho:YAG laser

IC pumped by a 2μm Tm:YAG laser, which in turn was excited by a 785nm Ti:sapphire laser[18]. The main justifications cited for using the IC pumping method, were: better mode coupling, lower thresholds, and increased efficiency particularly when the laser medium had a low absorption coefficient at the pump laser wavelength.

In this paper we report on IC pumped Er:YAG lasers where the Er:YAG crystal and the flash lamp pumped Er:glass rod share the same resonator mirrors. The IC pumped Er:YAG lasers operated in the $^4I_{13/2}$:Y3(6544cm$^{-1}$)-$^4I_{15/2}$:Z7(424cm$^{-1}$), 1.634μm transition at 300K. The IC pumping method offers several advantages over the standard outside cavity method of excitation. Namely, due to better mode matching of the Er:YAG laser to the Er:glass pump laser in the same resonator, better efficiency in utilization of the pump light is obtained. Furthermore, unlike the IC Yb,Er:glass lasers which suffer from limited power scaling due to the poor thermal conductivity of glass, the Er:YAG laser could have a much larger dynamic range of operating powers and energies.

This IC pumping method is particularly useful when pumping laser crystals with low absorption cross sections using a low intensity pump source[18]. In our particular case, the shifted Er:glass wavelength of 1.549μm (from the standard 1.532μm) has an absorption coefficient in Er:YAG: $\alpha_{1.549\mu m}$=0.059cm$^{-1}$ ($\alpha_{1.532\mu m}$=1cm$^{-1}$) per one percent $Er^{+3}$ concentration in YAG. Consequently, external laser pumping was not successful using the

1.549μm as the pump source. However, intra-cavity pumping at 1.549μm did yield 1.634μm laser action in Er:YAG crystals ranging in concentration from 0.3% to 2 % and 1cm to 8cm in length.

## Experimental Results

The Er:glass laser we used in this experiment consisted of a modified Quantronix model 210 power supply and laser head. The power supply was modified (by addition of extra capacitors in the pulse forming network) to produce 1.5ms long flash lamp pulses resulting in approximately 1.5ms long 1.549μm free running spiky outputs using an 80mm by 4mm diameter KIGRE Er:glass laser rod[19]. The close coupled single flash lamp laser cavity was modified to incorporate the KODAK White Reflectance Standard reflection coating in order to optimize flashlamp pump coupling in the $Yb^{+3}$ and $Nd^{+3}$ used as sensitizing co-dopants in the Er:glass rod. Our laser was air cooled because water cooling drastically reduced the output efficiency of the Er:glass laser. This is due to strong absorption of ≈1μm flashlamp radiation in water which reduces the excitation of $Yb^{+3}$ resulting in a reduced $Yb^{+3}$ to $Er^{+3}$ energy transfer (a major excitation mechanism for $Er^{+3}$, $Yb^{+3}$ in glass). Hence, we operated the Yb,Er:glass laser at a low repetition rate (≈ 0.02 Hz).

The measured spectral response of the mirrors used in our intra-cavity pumping arrangement are shown in Figure 1. It can readily be observed that the higher reflectivity at 1.549μm ($R_{1.549\mu}$=87%) versus 1.532μm ($R_{1.532\mu}$=78%) resulted in the Er:glass laser wavelength shift to 1.549μm. We achieved 1.549μm output power/energy close to those at the standard 1.532μm wavelength for the same flashlamp input level. Our Er:glass laser lased at two wavelengths simultaneously, regardless of which set of mirrors was used. Namely, when we utilized the 1.549μm mirrors, 1.549μm was the dominant wavelength in terms of output energies (approximately 40 times larger than the 1.532μm output). Conversely, when the standard 1.532μm mirrors were utilized, 1.532μm was the dominant wavelength with similar power ratios. It was demonstrated previously[11] that the Er:glass laser can oscillate at several different lines simultaneously provided it operates well above threshold.

We carried out a photoluminescence experiment on our Er:glass laser rod and the resulting spectra are shown in Figure 2 from which we note that the 1.549μm transition has approximately half the fluorescence intensity of the 1.532μm peak. It should be noted, however, that the gain ratio of the two competing transitions may not be proportional to their respective fluorescence intensity ratio due to different threshold inversion values (provided the transition linewidths are assumed equal). Our 1.549μm mirrors favored the 1.549μm transition, while

suppressing the inherently stronger competing 1.532μm transition.

Absorption measurements of Er:YAG using the 1.549μm Er:glass laser output (see Figure 3) were performed. The pulse to pulse energy stability of our Er:glass laser was better than 95%. The small signal absorption coefficient (per unit percent of Er concentration) was $\alpha_{1.549\mu m}=0.059cm^{-1}$. We repeated the absorption measurements with an Er:YAG crystal inside the Er:glass laser cavity. The absorption measurements showed the same value for $\alpha_{1.549\mu m}$, indicating that the 1.549μm Er:glass laser wavelength remained unchanged.

Wavelength determinations using a Jarrell Ash 0.25m monochromator for measuring the Er:glass wavelength with and without an Er:YAG crystal inside the cavity confirmed the above results. This is similar to the results of Anthon and Pier[15] who noted that the insertion of the Er:glass intra-cavity load into their Nd:YAG laser did not produce a wavelength shift in the Nd:YAG laser. In our case the lack of a wavelength shift, following the introduction of an IC Er:YAG load, can partially be explained with the aid of the Er:YAG absorption spectra (dashed curve) of Figure 4 (absorption spectra were obtained using a Varian CARY model 2415 spectrophotometer). Namely, since the 1.549μm line already lies well off of any sharp Er:YAG resonances, there is no strong selective loss which would otherwise force a shift in the laser oscillation wavelength. It should be noted that the magnitude of the 1.532μm energy in the Er:glass laser output was

sufficiently small (about 0.025 the strength of the 1.549μm output) such that it did not significantly affect the absorption measurements at the 1.549μm wavelength.

The Er:glass output wavelength shifts slightly depending on the voltage input to the flashlamp. Our measurements showed that a power supply input change of 30J (from 45J to 75J) shifted the peak of the Er:glass laser emission by approximately 3nm (from 1.535μm to 1.532μm when the standard 1.532μm mirrors were used). Since a similar shift was observed near the 1.549μm output when the 1.549μm mirrors were used, the power supply input to the flashlamp was kept fixed at 75J and the 1.549μm output was attenuated using a neutral density filter wheel for the absorption measurements. This insured that the Er:glass output wavelength remained fixed.

The intra-cavity lasing experimental arrangement is shown in Figure 5. The Er:YAG crystals (supplied by Scientific Materials Co.[20], and Union Carbide Corp.[21]) all lased at 1.634μm using the configuration of Figure 5. All crystals were polished flat-flat and uncoated. Fixing the pump at the input level of 75J corresponding to that used for all the external absorption measurements facilitated a quantitative comparison of energy absorbed in the Er:YAG crystals pumped intra-cavity. However, our Er:glass laser was operated near its maximum stable output, thus, we were unable to obtain data at a higher power input. The temporal 1.634μm laser signal together with the 1.549μm pump laser signal is shown in Figure 6. It should be noted that the

intensity of the 1549μm signal was much stronger than the 1.634μm such that the 1.549μm monitoring detector did not require a notch filter.

The threshold energies were obtained from the temporally resolved integrated 1.549μm Er:glass laser pulse and the corresponding 1.634μm laser onset delays. The integration was achieved digitally utilizing an HP 54510A digitizing oscilloscope interfaced to an IBM XT computer. A typical spiked laser output and the corresponding integrated pulse is shown in Figure 7. At the fixed 75J power supply input, the available 1.549μm energy in the absence of any IC load was 150mJ. Hence, the temporally integrated 1.549μm pulse provided an accurate determination of how much energy is delivered at any point in time. The energy absorbed was then determined fractionally from the temporally integrated signals and the total energies absorbed in the crystals as determined from equation 3 in the Theoretical Analysis section. These results are listed in Table 1 for the four Er:YAG crystals utilized in these experiments.

Direct measurement of the 1.634μm energy was difficult because of the relative spectral closeness of the 1.549μm and the 1.634μm outputs in the presence of the much stronger 1.549μm signal. Direct 1.634μm energy measurement would require a notch filter with an exceptionally high (>200) 1.634μm to 1.549μm rejection ratio. Our notch filter had a 1.634μm to 1.549μm rejection ratio of approximately 40, thus, it only

partially attenuated the 1.549μm signal. Therefore, the strength of the 1.634μm signal was determined indirectly by the use of the monochromator-detector combination calibrated with the outside cavity 1.532μm pumped 1.645μm Er:YAG laser[8]. These results are listed in Table 1.

The 1% and 2% 1cm long Er:YAG crystals lased in the intra-cavity pumping configuration in the absence of the 15cm focal length lens. The longer crystals (3.8cm and 8cm), however, could not be made to lase without the lens. The data of Table 1 lists our results. The threshold values for the 1cm long crystals are in reasonable agreement with theory, whereas the measured values for the longer crystals are several times larger than the theoretical estimates. This is most likely due to the variation of the 1.549μm pumping filament diameter of a longer Er:YAG crystal versus a shorter one.

Burn spot measurements (on Polaroid 667 film) of the focused 1.532μm Er:glass laser beam (outside the cavity with the 1.532μm flat-flat mirror set, using our 15cm focal length lens) yielded a Full Width Half Maximum (FWHM) spot size of ≈800μ. We then measured the diameter of the beam just outside the output coupler with the 1.549μm mirror set (semi-confocal cavity) and obtained a FWHM of ≈600μm. Using this technique, and from the relative f# change (from 2mm diameter non-focused beam to 800μm focused beam) of our 15 cm lens (empirically determined), we estimated the size of the focused spot in the intra-cavity Er:YAG crystal to be approximately 240μm.

From Table 1 we note that the intra-cavity 1.634μm Er:YAG laser action was achieved with a minimum product of the absorption coefficient and crystal length of $\alpha L=0.059$ (1cm long 1% Er:YAG crystal). Although the 0.5% Er:YAG 1cm long crystal lased with the highest efficiency when pumped outside cavity by the 1.532μm ($\alpha_{1.532\mu m}=1cm^{-1}$) Er:Glass laser[8], it did not lase at all in the intra-cavity pumping configuration. With an $\alpha L_{1.549\mu}=0.03$, there was insufficient absorption in the 0.5% Er:YAG 1cm long crystal to lase intra-cavity. This result was predicted by our theoretical threshold calculations for lasing crystals with the same parameters.

We achieved IC laser action in a 8cm long 0.5% Er:YAG crystal, although with low outputs. That is for the same pump inputs and lasing conditions, the IC 1.634μm laser action in the 8cm long 0.5% Er:YAG crystal manifested itself in a few spikes, barely operating above threshold. This crystal had the highest $\alpha L(=0.24)$, which introduced too much absorption for efficient intra-cavity operation.

## Theoretical Analysis

The energy level diagram for Er:YAG at 300K is shown in Figure 8 showing the pump and lasing transitions for the intra-cavity (solid lines) and the external cavity (dashed lines) experiments together with the calculated Boltzmann factors. In comparing the 1.645μm and the 1.634μm transitions, one notes

that the Boltzmann factor inversion ratio is more favorable for the 1.645μm ( $\frac{y3}{z7}$ =9.45 versus 1.634μm ($\frac{y1}{z6}$ =7.75).

Furthermore, the mirror spectral response (Figure 1) does not favor the 1.634μm wavelength over the standard 1.645μm. However, as can be seen from the absorption spectra of Nd:glass (Figure 9), the 1.645μm is lossier than 1.634μm in terms of the relative absorption by $Nd^{+3}$ in the Er:glass laser rod. Hence, it is likely that the $Nd^{+3}$, which is present as a co-dopant in the KIGRE Er:glass laser rod forces the Er:YAG crystals to lase at the 1.634μm wavelength.

Following the treatment of Rabinovich et al[16], we calculate the energy absorbed in the IC Er:YAG lasers from the small signal absorption coefficient, α, ( measured outside the cavity to be $\alpha_{1.549\mu m}=0.059cm^{-1}$, per unit % Er concentration)

$$E_{abs}=E_{cav}\{(1-e^{-\alpha L})+re^{-\alpha L}(1-e^{-\alpha L})+r^2e^{-2\alpha L}(1-e^{-\alpha L})$$

$$+r^3e^{-3\alpha L}(1-e^{-\alpha L})+...\}, \qquad (1)$$

which for αL«1 (coinciding with our regime) can be written as

$$E_{abs}\approx E_{cav}\{\alpha L+\alpha L[1-\alpha L]r+\alpha L([1-\alpha L]r)^2$$

$$+\alpha L([1-\alpha L]r)^3+...\} \qquad (2)$$

where $E_{abs}$ is the total energy absorbed in the IC laser crystal for an infinite number of passes, $E_{cav}$ is the total available pump energy in the cavity, and L is the crystal length. r is the effective output coupler reflectivity which includes all cavity losses (per pass) other than absorption in Er:YAG. For high reflectivities (small output coupling, $t=1-r<<1$) and low single pass absorption of the IC laser, equation (2) becomes

$$E_{abs}=E_{cav}\frac{\alpha L}{(1-r+r\alpha L)}=E_{cav}\frac{\alpha L}{(t+\alpha L-t\alpha L)}, \qquad (3)$$

which can be approximated as

$$E_{abs}\approx E_{cav}\frac{\alpha L}{(\alpha L+t)} \qquad (4)$$

where t here represents all cavity losses per pass (including the output coupling losses) with the exception of Er:YAG absorption, $\alpha L$. These losses include bulk and surface scattering, and diffraction. We measured the 1.549μm reflection losses at the Er:YAG surfaces to be ≈10% (which agrees with the theoretically predicted value (using the refractive index, n=1.82) of 9%, thus giving $\delta=0.17$.(our Er:YAG crystals were not AR coated).

Assuming negligible diffraction and bulk scattering losses we calculated the total energy absorbed in the IC Er:YAG crystals to be: $E_{abs}$ = 22.4, 44.3, 42.4, and 51 mJ for crystals 1 through 4 respectively, where we used the theoretical lasing threshold absorbance values, $\alpha L$, in these calculations. These values were then used to obtain the experimental threshold energies (see Table 1). As mentioned earlier, the power supply input was kept constant at 75J providing a constant $E_{cav}$=150mJ in the absence of any IC load.

The analysis of the lasing efficiency in an intra-cavity pumping configuration is difficult because of the non-linear pumping process of the Er:YAG crystals. However, we estimated the pumping efficiency using conventional laser theory outlined below. The expression for the output intensity as a function of the input in the small output coupling approximation is[22]

$$I_{out}= \frac{I_S T}{2} \left(\frac{2\gamma L}{T+\delta} -1\right) \qquad (5)$$

where $I_S= \frac{h\nu}{\sigma\tau}$ is the saturation intensity, T is the output coupler transmittance, $\gamma$ is the small signal gain coefficient, L is the crystal length, $\sigma$ is the stimulated emission cross-section, $\tau$ is the upper level lifetime, and $\delta$ represents additional cavity losses per round trip. Since our IC laser operated in a quasi-cw mode during the duration of the pump pulse, equation (5) is applicable

to our case. Differentiating (5) with respect to T and setting it to zero allows one to calculate the optimum output coupling, $T_{opt}$, such that the output intensity is a maximum. Performing this calculation yields

$$T_{opt}=\delta\left(\sqrt{\frac{2\gamma L}{\delta}}-1\right) \qquad (6)$$

Using this analysis, Rabinovich et al[16] modified relation (6) to give the optimum absorption in an I/C laser as [23]

$$\alpha L_{opt}=t\left(\sqrt{\frac{g}{t}}-1\right) \qquad (7)$$

where t, as before, represents all the losses in the cavity (including the output coupling) except for the Er:YAG absorption, and g is the small signal gain defined as

$$g=2\gamma L, \qquad (8)$$

where the small signal gain coefficient, $\gamma=\sigma\Delta N_{th}$ , $\sigma$ being the stimulated emission cross-section and $\Delta N_{th}$ the threshold inversion density. From Er:YAG fluorescence

spectra (Figure 4: solid curve) and the previously determined[24] 1.645μm stimulated emission cross-section, we calculated the 1.634μm stimulated emission cross-section to be $1 \times 10^{-20}$ $cm^2$. Then, from the threshold inversion densities corresponding to cavity losses of T=0.05 and δ=0.17, we calculated the optimum absorption coefficient-crystal length product to be $\alpha L^{opt}_{1.549\mu m}=0.0875$.

In order to compare the experimentally determined thresholds with the theoretically calculated ones we proceeded as follows: the threshold for laser action is approximately given by

$$R_1 R_2 e^{2(L\Delta N\sigma-\delta)}=1 \qquad (9)$$

where $R_1$,$R_2$ are the mirror reflectivities, $\Delta N$ is the population inversion, $\sigma$ is the stimulated emission cross section , L is the crystal length and δ represents losses in addition to the output mirror. δ includes surface and bulk scattering losses per pass. Solving for $\Delta N_{th}$ gives

$$\Delta N_{th}=\frac{\delta}{\sigma L}+\frac{1}{2L\sigma}\ln\left(\frac{1}{R_1 R_2}\right). \qquad (10)$$

Then, since the 1.634μm laser action occurs between the Stark levels y1 and z6, we can write the threshold condition as

$$N_{y1}-N_{z6}=\Delta N_{th}, \qquad (11)$$

where the Stark levels are defined in terms of the total manifold populations ($y:{}^4I_{13/2}$, $z:{}^4I_{15/2}$) as

$$N_{y1}=\frac{f_{y1}}{Z_y}N_y \ , \ N_{z6}=\frac{f_{z6}}{Z_z}N_z \qquad (12)$$

$f_{y1}$,and $f_{z6}$ are the appropriate Boltzmann factors (see Figure 8) and the partition functions are:

$$Z_{y,z}=\sum_{i=1}^{(7,8)} e^{-\frac{\Delta E_i}{kT}} \qquad (13)$$

Thus, using (12) we calculated the population densities, $N_y$ and $N_z$ at threshold and assuming that each excited ion in ${}^4I_{13/2}$ represented one absorbed 1.549μm photon, we calculated the energy required to reach threshold (using corresponding pumped volumes in each crystal). This assumption is valid because the

$^4I_{13/2}$ lifetime (≈7ms) is long compared to ≈200μs required to reach threshold. In these calculations, δ was set at the previously determined value of 0.17 (assuming only surface reflection losses), and using the Boltzmann factors (Figure 8), and the mirror reflectivity values (Figure 1), the threshold inversion density was calculated from $\Delta N_{th}=\frac{1.95\times10^{19}}{L}$ $cm^{-3}$. The resulting calculated thresholds are listed in Table 1.

The results of Table 1, indicate reasonably good agreement between the absolute values of the calculated versus the experimentally determined threshold values for the 1cm long crystals (1 and 2). The large discrepancy in the theoretical versus experimental threshold values for the long crystals (3 and 4) was attributed to an increased spatial inhomogeneity of the pumped volume in the long (L»1cm) crystals. Namely, our estimate of the pumped volume was too small.

## Conclusions

Laser action in Er:YAG at 1.634μm pumped in an intra-cavity configuration by an Er:glass laser operating at 1.549μm is reported. The selective 1.634μm lasing (over the 1.645μm) is most likely due to higher absorption of the 1.645μm wavelength by the Nd co-dopant in the Er:glass rod, and is probably unique in this IC pumping arrangement. The Er:glass laser was shown to work efficiently at the shifted 1.549μm wavelength (a new wavelength in Er:glass) by utilization of cavity mirrors with suitable reflectivity spectra.

## Acknowledgements

We thank Mr. John D. Myers, president of Kigre Inc., for the generous gift of the Er, Yb:phosphate glass laser rods used in this work.

The authors are grateful to Ralph Hutchinson of Scientific Materials Co. for supplying us with the 1cm long crystals of Er:YAG.

The authors are grateful to Milan Kokta of Union Carbide Corp. for supplying us with the long (3.8-8cm) Er,Yb:YAG laser rods.

## References


1. Z.J.Kiss and R.C.Duncan Jr. ,"Optical Maser Action in $CaWO_4:Er^{+3}$" Proc. IRE **50**,1531 (1962)

2. S.A.Pollack, "Stimulated Emission in $CaF_2:Er^{+3}$", Proc. IEEE **51**,1793-1794 (1963)

3. W.F.Krupke and J.B.Gruber, "Energy Levels of $Er^{+3}$ in $LaF_3$ and coherent emission at 1.61μ", J.Chem. Phys.**41**(5),1225-1232 (1964)

4. L.F.Johnson, J.E.Geusic and L.G.VanUitert, "Coherent Oscillations from $Tm^{+3}$, $Ho^{+3}$, $Yb^{+3}$, and $Er^{+3}$, ions in Yttrium Aluminum Garnet", Appl.Phys.Lett. 7(5),127-129(1965)

5. K.O.White and S.A.Schleusener, "Coincidence of Er:YAG laser emission with methane absorption at 1645.1nm", Appl.Phys.Lett. **21**,419-420 (1972)

6. G.Huber, E.W.Duczynski, and K.Petermann, "Laser pumping of Ho-, Tm-, Er-doped Garnet lasers at room temperature", IEEE J.Quant. Electron. **24**(6),920-923 (1988)

7. H.Stange, K.Petermann, G.Huber, and E.W.Duczynski, "Continuous wave 1.6μ laser action in Er-doped garnets at room temperature", Appl.Phys.B **49**,269-273 (1989)

8. K.Spariosu and M. Birnbaum, "Room temperature 1.645 micron Er:YAG lasers", OSA Proc. on Advanced Solid-State Lasers, Feb.17-19, Santa Fe, New Mexico, 127-130 (1992).

9. G.M.Zverev, V.M.Garmash, A.M.Onishchenko, V.A.Pashkov, A.A.Semenov, Yu.M.Kolbatskov, and A.I.Smirnov, "Induced emission by trivalent erbium ions in crystals of yttrium-aluminum garnet", J.Appl.Spectrosc.(USSR), **21**,1467-1469(1974).

10. A.A.Kaminskii, "Laser Crystals", 2nd. ed. (Springer-Verlag, New-York, 1990) pg.143.

11. V.P.Gapontsev,M.E.Zhabotinskii,A.A.Izyneev,V.B. Kravchenko, and Yu.P.Rudnitskii, "Effective 1.054-1.54μ stimulated emission conversion", JETP Lett. **18**,251-253 (1973)

12. V.N.Kalinin, A.A.Mak, D.S.Prilezhaev, and V.A.Fromzel' "Lasing properties of $Yb^{+3}$ and $Er^{+3}$ glass laser pumped by a laser", Sov.Phys.Tech.Phys. **19**(6),835-836(1974)

13. A.G.Murzin and V.A.Fromzel', "Maximum gains of laser-pumped glasses activated.with $Yb^{+3}$ and $Er^{+3}$ ions", Sov.J.Quantum Electron. **11**(3),304-308 (1981)

14. R.G.Aubakirov, A.G.Murzin, and V.A.Fromzel, "Raising the efficiency of intracavity laser pumping of selectively absorbing media", Opt.Spectrosc.(USSR) **55**(3),295-298 (1983)

15. D.W.Anthon and T.J.Pier, "Diode-pumped Erbium glass lasers", SPIE Proc. Solid-State Lasers III (1992), pg.8-12.

16. W.S.Rabinovich, S.R.Bowman, B.J.Feldman, and M.J.Winings, "Tunable Laser pumped 3μ Ho:$YAlO_3$ laser", IEEE J.Quantum Electron. **27**(4),895-897 (1991)

17. S.R.Bowman and B.J.Feldman, "Demonstration and analysis of a Ho quasi-two level laser", SPIE Proc. Solid-State Lasers III (1992), pg.46-54.

18. R.C.Stoneman and L.Esterowitz, "Intracavity-pumped 2.09μ Ho:YAG laser", Opt.Lett. **17**(10), 736-738(1992).

19. P.W.Milonni and J.E.Eberly, "Lasers" (J.Wiley and Sons, New York,1988), pg.324.

20. A.Siegman, "Lasers", University Science Books (Mill Valley, CA, 1986),pgs.477-479.

21. D.K.Killinger, "Phonon-assisted upconversion in 1.64μ Er:YAG lasers", LEOS Digest of Tech. Papers, Apr.26,1987, pg.240.

## Figure Captions

Table 1. Intra Cavity 1.549μm pumped 1.634μm Er:YAG laser performance.

Figure 1. Output coupler (mirror B1) spectrally resolved reflectivity.

Figure 2. KIGRE Er:glass laser rod photoluminescence spectra.

Figure 3. Experimental arrangement for absorption measurements.

Figure 4. Er:YAG absorption (dashed curve) and photoluminescence (solid curve) spectra.

Figure 5. Intra-cavity laser pumped lasing arrangement.

Figure 6. Temporal 1.634μm laser signal relative to the 1.549μm pump signal (horizontal scale: 200μs per division; vertical scale: arbitrary).

Figure 7. Free-running and the corresponding temporally integrated Er:glass laser outputs.

Figure 8. Energy level diagram for Er:YAG (300K).

Figure 9. Nd:glass absorption spectra.

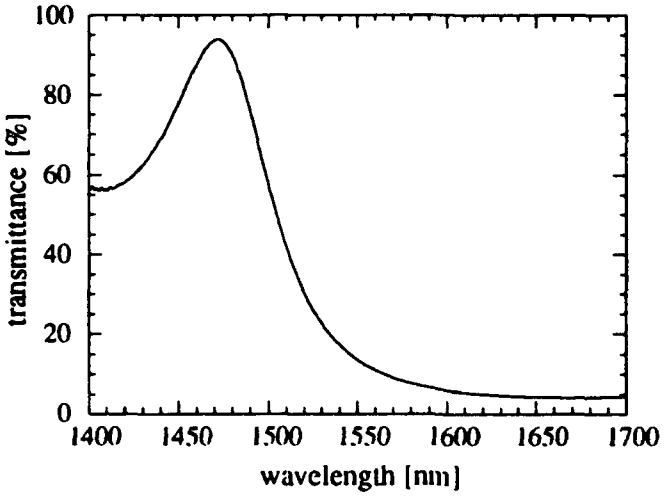


Figure 1: Output coupler (mirror B1) spectrally resolved reflectivity

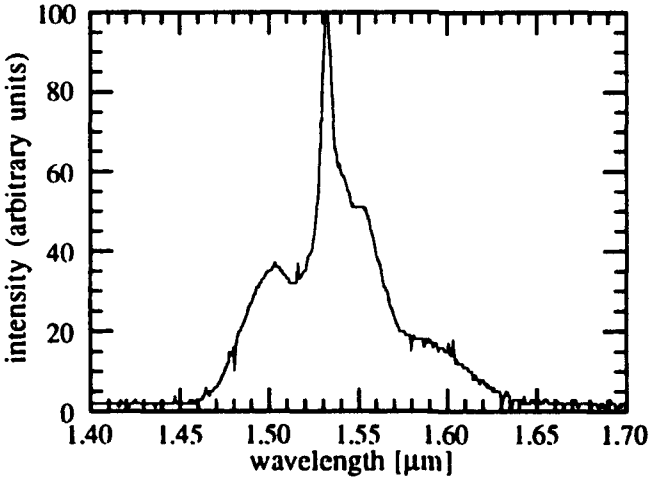


Figure 2: KIGRE Er:glass laser rod photoluminescence spectra

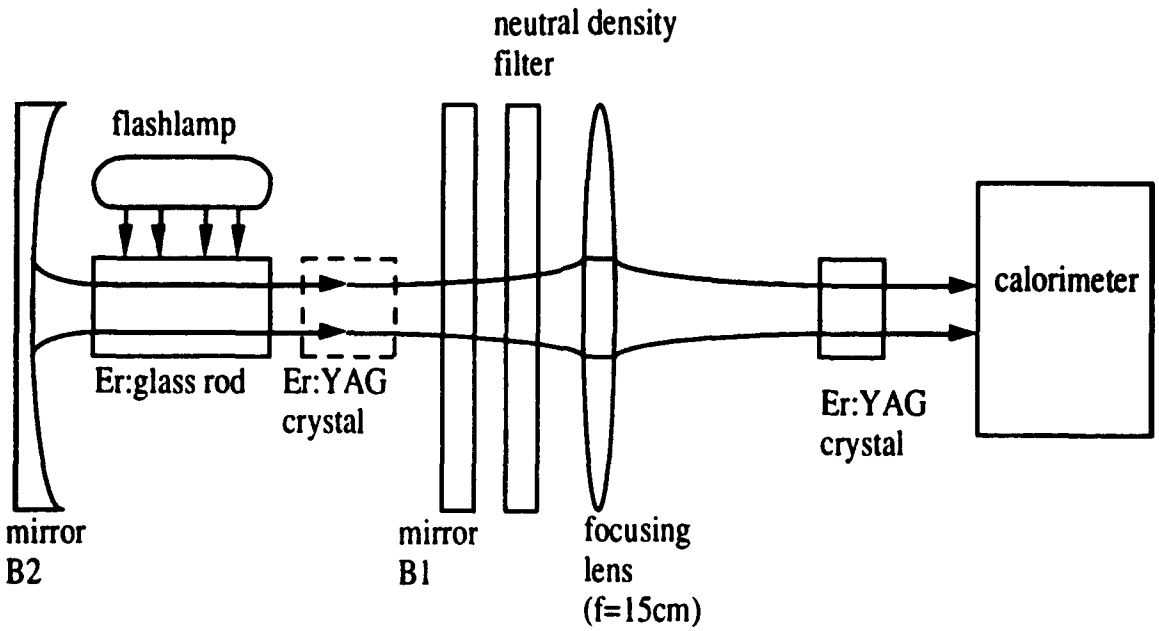


Figure 3. Experimental arrangement for aborption measurements

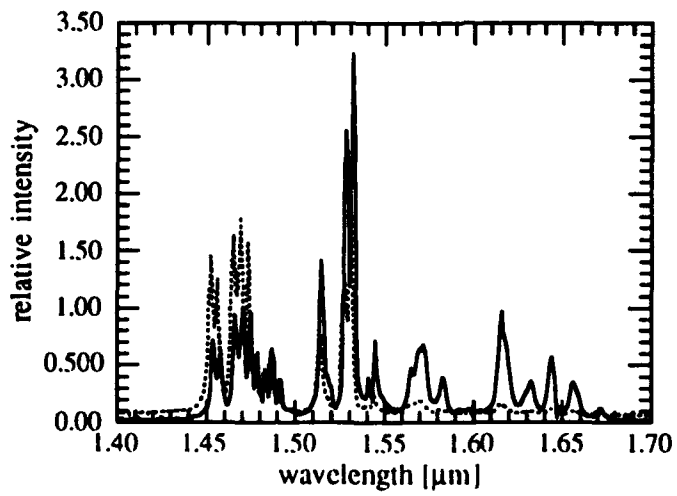


Figure 4. Er:YAG absorption (dashed curve) and photoluminescence (solid curve) spectra

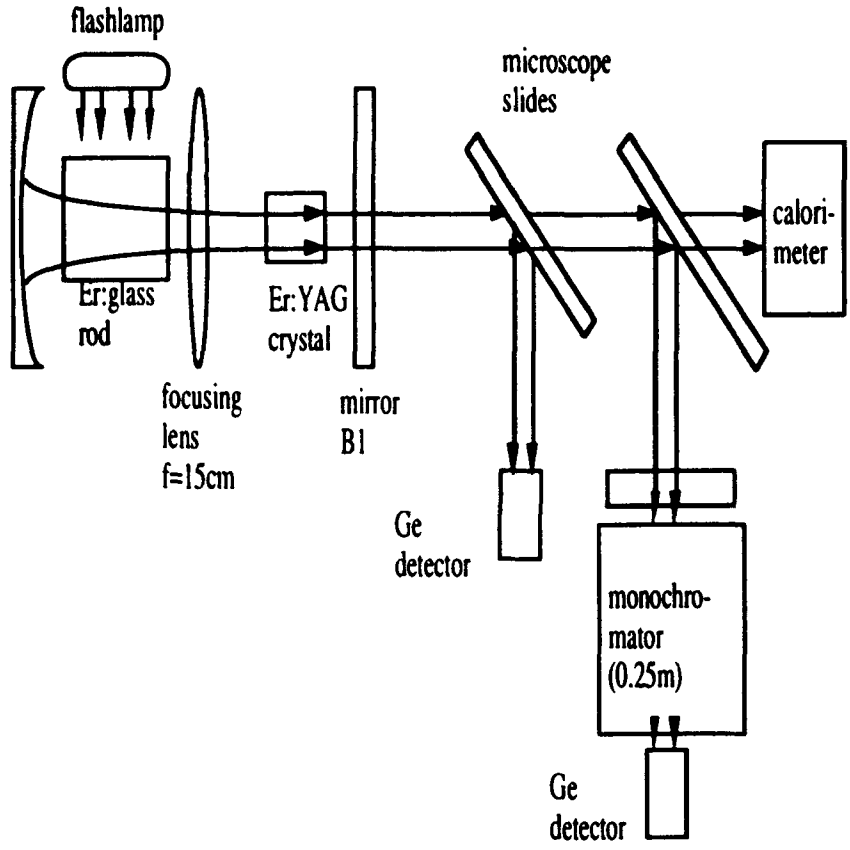


Figure 5. Intra-cavity laser pumped lasing arrangement

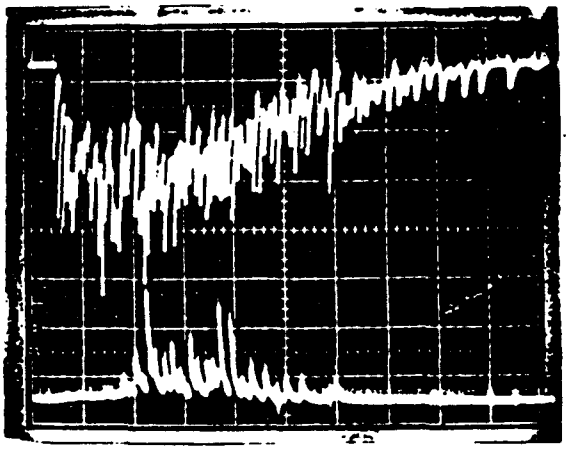


Figure 6. Temporal 1.634μm laser signal with the relevant 1.549μm pump signal (horizontal scale: 200 μm per division; vertical scale: arbitrary).

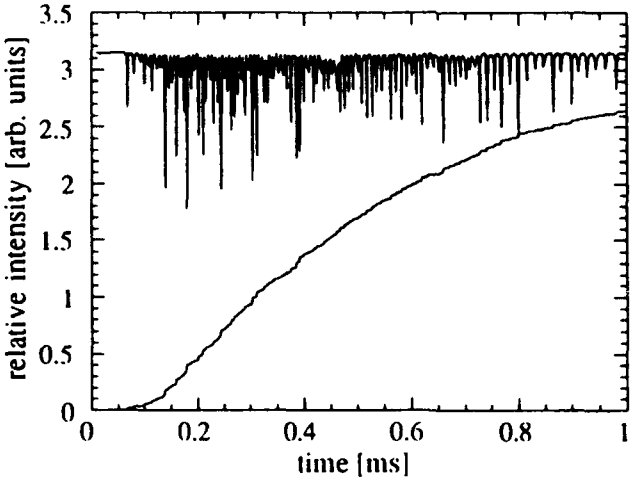


Figure 7: Free running and the corresponding temporily integrated Er:glass laser outputs

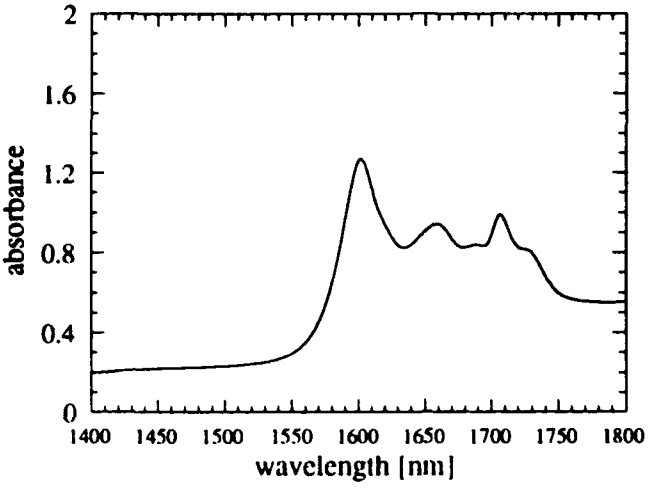


Figure 9: Nd:glass absorption spectra

TABLE I. INTRA-CAVITY 1.549μm PUMPED 1.634μm Er:YAG LASER PERFORMANCE

| Er:YAG Crystal | Er [%] | Length [cm] | $(\alpha L)^{0}_{1.549\mu m}$ | $(\alpha L)^{th}_{1.549\mu m}$ | Experimental $E_{th}$ [mJ] | ratio | Theoretical $E_{th}$ [mJ] | ratio | 1.634μm output [mJ] |
|---|---|---|---|---|---|---|---|---|---|
| 1 | 1 | 1 | 0.06 | 0.039 | 4.5 | 1.0 | 2.89 | 1.0 | 1.6 |
| 2 | 2 | 1 | 0.12 | 0.092 | 6.2 | 1.38 | 3.78 | 1.308 | 1 |
| 3 | 0.5 | 3.8 | 0.114 | 0.087 | 22.6 | 5.02 | 3.70 | 1.28 | 4 |
| 4 | 0.3 | 8 | 0.144 | 0.114 | 28 | 6.22 | 4.14 | 1.43 | 3.2 |

# $Er^{3+}:Y_3Al_5O_{12}$ Laser Dynamics: Effects of Upconversion

by:

Kalin Spariosu, and Milton Birnbaum

University of Southern California
Center for Laser Studies
University Park, DRB B17
Los Angeles, CA 90089-1112,

and

Bruno Viana
Lab. de Chimie Appl. de l'Etat Solide
Universite Pierre et Marie Curie
Ecole Nationale Superieure de Chimie de Paris
11, rue Pierre et Marie Curie
75231 Paris Cedex 05, France

ABSTRACT

Room temperature 1.532μm pumped 1.645μ laser action in the $Er^{3+}$:$Y_3Al_5O_{12}$ (Er:YAG) $^4I_{13/2}y3(6602cm\text{-}1) \Rightarrow$ $^4I_{15/2}z7(523cm^{-1})$ transition was demonstrated and analyzed. Laser action at 1.645μm was achieved in Er:YAG crystals with Er concentrations ranging from 0.5% to 4%. Slope efficiencies as high as 40% were obtained with 0.5% Er:YAG. For concentrations up to 4% measurements of laser thresholds indicated that upconversion losses were small.

## INTRODUCTION

The first 1.6μm $^4I_{13/2}$-$^4I_{15/2}$ laser action was demonstrated in Er:$CaWO_4$[1]. Laser action in Er:$CaF_2$[2], and in Er:$LaF_3$[3] near 1.6μm for both crystals was subsequently reported. Flash lamp pumping at 77K was utilized in all cases. The first 1.645μm $^4I_{13/2}$-$^4I_{15/2}$ laser action in Er:YAG was achieved by Johnson et al[4] at 77K, and later at room temperature by White and Schleusener[5], again using flash lamp excitation in both cases. More recently, CW oscillation at 1.645μm in Er:YAG was achieved using a Kr ion laser at 0.647μm in an end pumping arrangement[6,7]. We reported 1.532μm pumped 1.645μm Er:YAG lasers at 300K using an Er:glass laser as the pump source in an end pumped configuration[8]. All of the above reported Er:YAG lasers at 300K oscillated in the $^4I_{13/2}$:Y3(6602$cm^{-1}$)⇒$^4I_{15/2}$:Z7(523$cm^{-1}$) transition at 1.645μm. Zverev et al[9] reported on a flash-lamp pumped 1.632±2μm Er:YAG laser action at 300K. The authors did not discuss mechanisms for this shift from the standard 1.645μm laser line.

The recent revival of interest in the Er lasers at 1.6μm stems from the desirability of eye-safe lasers operating within an atmospheric window and, thus, potentially useful for atmospheric sounding and numerous other applications. A diode pumped version would have the advantages of high efficiency, reliability, and compactness. Killinger studied the potential

capability of the 1% Er:YAG 1.64μm laser utilizing pumping at 1.47μm. Killinger found a much higher threshold than that predicted theoretically and reached a preliminary conclusion that upconversion losses were the primary factor. To resolve this potential problem, we studied upconversion effects in Er:YAG crystals and obtained detailed threshold measurements to identify possible upconversion losses. It is well known that upconversion via cooperative non-radiative energy transfer is an important mechanism for the excitation of upper lying energy levels of rare earth ions in crystalline hosts, particularly for high dopant concentrations. There are several excellent review articles on this topic[10,11,12]. In $Er^{3+}$:crystals and glasses, the cooperative energy transfer is a major excitation mechanism for achieving laser action from the upper lying states. In fact, upconversion pumped laser action was achieved using 1.5μm excitation through both di-ionic[13,14,15] and tri-ionic[16,17,18] energy transfer (see Figure 1). In the low concentration regime, ≤ 4%, only ion pair upconversion processes need be considered in $Er^{3+}$:YAG.

Recent work[19] supports our results that for low concentrations of Er in YAG upconversion losses are low. McFarlane et al. showed that in 5% Er:YLF the pair upconversion loss contribution from the $^4I_{13/2}$ level is about 4%. Measurements on Er:YAG by McFarlane et al.[19] were taken only for 33%Er:YAG. However, if we utilize the results obtained by

Zhekov et al.[20], we find that the upconversion losses in 5%Er:YAG would be no greater than that reported for 5%Er:YLF.

Our focus in this work was to demonstrate by detailed measurements of low concentration Er:YAG lasers and theoretical analysis of our results that the Er:YAG laser performance was consistent with small upconversion losses. Our results for the laser thresholds showed good agreement with theoretical modeling where we assumed no upconversion losses. Only the 0.5% Er:YAG laser operated with high slope efficiency. We believe that the lower slope efficiencies observed with the higher Er concentration Er:YAG lasers could have been caused by poor overlap of the pump and laser beams in our end-pumping arrangement.

## EXPERIMENTAL RESULTS

The Er:glass laser we used in this experiment consisted of a modified Quantronix model 210 power supply and laser head. The original pulse forming network (PFN) of the Quantronix power supply provided approximately a 1ms long flash lamp pulse resulting in a free-running (spiking) 1.532μm output approximately 1ms in duration from a 4mm DIA x 80mm long KIGRE QE7 Er:glass laser rod. The PFN consisted of six 30μf capacitors for a total of 180μf. The Er:glass laser resonator consisted of two plane parallel mirrors. The transmittance of the output coupler (T≈15%) was practically constant over a 50nm wavelength range centered at 1.53μm. Energy output performance at 1.532μm is shown in Figure 2. This power supply (with the 180μf PFN) was used as the pump source in the upconversion fluorescence measurements.

The power supply was subsequently modified (by the addition of 90μf to the PFN ) to produce 1.5ms long flash lamp pulses resulting in approximately 1.5ms long free running spiky 1.532μm outputs where most of the energy is concentrated in the relatively flat first 1ms of the pulse. The close coupled single flash lamp laser cavity was modified to incorporate the KODAK White Reflectance Standard reflection coating in order to optimize flashlamp pump coupling in the $Yb^{+3}$ and $Nd^{+3}$ used as sensitizing co-dopants in the Er:glass rod. Our laser was air cooled because water cooling drastically reduced the output

efficiency of the Er:glass laser. This is due to strong absorption of ≈1μm flashlamp radiation in water which reduces the excitation of $Yb^{+3}$ resulting in a reduced $Yb^{+3}$ to $Er^{+3}$ energy transfer (a major excitation mechanism for $Er^{+3}$, $Yb^{+3}$ in glass). Thus, we could operate the Yb,Er:glass laser only at a low repetition rate (≈ 0.02 Hz).

It was demonstrated previously[19] that the Er:glass laser can oscillate at several different lines simultaneously provided it operates well above threshold. Our laser, which utilized a KIGRE QE-7 phosphate glass, lased at two wavelengths simultaneously: 1.532μm and 1.549μm. However, the 1.532μm wavelength was dominant with approximately 40 times greater output energy than the 1.549μm wavelength. Wavelength measurements of our Er:glass laser were carried out using a Jarrell-Ash 82-497 monochromator. The Er:glass output wavelength shifted slightly depending on the voltage input to the flashlamp. Measurements showed that a power supply input change of 30J (from 45J to 75J) shifted the peak of the Er:glass laser emission by as much as 3nm (from 1535nm to 1532nm). Therefore, when carrying out absorption bleaching measurements, the power supply input to the flashlamp was kept fixed at 75J in order to insure that the Er:glass output wavelength remained fixed.

The spectral absorption data were obtained with a Varian CARY model 2415 spectrophotometer and digitally stored in an IBM PC allowing us to transfer it to a MacIntosh computer for

plotting. The absorption spectra obtained for 1%Er:YAG is shown in Figure 3. There is some absorption at the 1.645μm laser wavelength which is expected from the population of the lower level at room temperature. However, this absorption is small compared to the absorption at 1532nm. The small signal absorption coefficient at 1.532μm, $\alpha(1\%Er)=1cm^{-1}$, was determined using the Er:glass laser at 1.532μm as the pump, and was confirmed by the CARY measured value (Figure 3). Thus, for a sample length of 1cm, $\alpha L=1$ for 1%Er:YAG at 1.532μm.

Absorption (and bleaching) measurements using the Er:glass laser source were performed using the experimental arrangement of Figure 4. The energy meter used was Scientech 365 (and in some instances, Laser Precision RJ7200). The attenuation of the Er:glass laser beam was achieved without compromising its spectral and temporal integrity by the utilization of a calibrated neutral density filter wheel. The absorption bleaching measurements were computed using the definition of the time integrated (total) absorption coefficient as $\alpha=\frac{\ln(\frac{E_{out}}{E_{in}})}{L}$ (absorbance=αL). Figure 5 shows the bleaching results. The observed bleaching agrees well with the theoretical models.

In order to temporally resolve the amount of energy absorbed during the duration of the pump pulse, we carried out a modified bleaching experiment where we monitored the input

and the output pulses to the sample simultaneously using an identical pair of detectors. The digitized spiking signals were subsequently numerically integrated in the IBM PC by simply adding consecutive data points. The result is a temporally resolved increasing energy as a function of time. An example of spiking and the corresponding integrated signals is shown in Figure 6.

Our photoluminescence data was obtained using a computer controlled Jarrell-Ash Czerny-Turner 1m scanning spectrometer interfaced to an IBM PC where the fluorescence data was digitally stored. This allowed for computer graphics plotting using a MacIntosh computer (similar to the absorption data processing). The detection was achieved with a North Coast Scientific EO817L cooled Ge detector, while the excitation was done with a chopped output from a LEXEL Model 95 Argon Ion laser at 514nm. Photoluminescence spectra for Er:YAG is shown in Figure 3. The 1.645μm laser emission peak is clearly identified in Figure 3.

The upconversion fluorescence data was obtained utilizing the experimental arrangement of Figure 7. The exit slit of the Jarrell-Ash 82-497 monochromator was interfaced with a Hamamatsu R632 photomultiplier tube (PMT) with an S1 photocathode. This enabled us to detect fluorescence in the visible wavelength range as well as near infrared emission ≤ 1μm. The 1.532μm pump reference was detected simultaneously using an InAs detector. Signals from both the

PMT and the InAs detector were recorded using a Tektronix 7844 dual beam oscilloscope.

We monitored upconversion fluorescence from 4 different transitions in Er:YAG: $^4I_{11/2}$-$^4I_{15/2}$ (980nm), $^4F_{9/2}$-$^4I_{15/2}$ (670nm), $^4S_{3/2}$-$^4I_{15/2}$ (550nm), and $^2H_{9/2}$-$^4I_{15/2}$ (410nm). Figure 8 shows the temporal correlation between the input 1.532μm pulse and the corresponding 980nm signal (the initial bump is some leakage of flash lamp light). All of the spectrally and time resolved upconversion fluorescence traces were obtained using the monochromator. Intensity curves were not corrected for the different wavelength responses of the spectrometer and the different neutral density filters employed. When viewing spectrally integrated fluorescence in the absence of a monochromator and using a Si detector, the 980nm signal was the dominant in intensity (as expected). The 980nm upconversion fluorescence is shown in Figure 8 for different Er doping concentrations in YAG.

The upconversion build up time is roughly 600μs; namely, the peak upconversion fluorescence occurs about 600μs after the onset of the 1.532μm pump radiation. (The decay time after the cessation of the 1.532μm pump pulse is governed by the inherent lifetimes of the respective energy levels in Er:YAG). In our Er:YAG laser experiments threshold occurred usually about 200μs after the onset of the pump radiation implying lower upconversion losses as compared to those corresponding to peak fluorescence intensities shown in Figure 8. In subsequent

sections of this paper, we show that the observed laser oscillation thresholds for <4%Er:YAG lasers are in good agreement with the theoretically predicted thresholds, where upconversion losses are excluded from the calculations.

The characterization of the 1.532μm end-pumped Er:YAG laser emission at 1.645μm involved temporal output measurements, as well as the direct measurement of the total 1.645μm energy for a given 1.532μm input. The Er:glass pump laser operated single-shot at a low repetition rate (≈0.02Hz) and its output was a series of pulselets, (spikes) characteristic of free-running solid-state lasers. Therefore, it was necessary to simultaneously monitor the temporal 1.532μm input trace, the 1.645μm laser output trace, and the energy transmitted through the sample.

The experimental arrangement for the temporal 1.645μm laser diagnostics is shown in Figure 9. The input to the sample was determined by measuring the transmittance of each optical component, inclusion of the surface reflection losses, and by calibrating the neutral density filters prior to carrying out the experiment. In order to separate the 1.645μm output from the stronger Er:glass pump at 1.532μm, a notch filter (1.532μm to 1.645μm rejection ratio of 60 to 1) was used. The 1.645μm signal was sampled out of output coupler (T≈5% at 1.645μm), counter-propagating with respect to the 1.532μm pump. Furthermore, the small reflection (R≈10%) at 1.532μm from the 1.645μm output coupler provided for a higher 1.645μm to

1.532μm rejection ratio than would be available with T≈50% at 1.532μm of the 100% 1.645μm reflector in a co-propagating signal detection mode. All the laser resonator mirrors utilized in this experiment were plane-parallel with radius of curvature, $R_C \approx \infty$.

The power supply of the Er:glass laser was kept at a fixed input in order to maintain the temporal and spectral integrity of the 1.532μm pump pulse. The temporal 1.532μm and the 1.645μm lasing traces were recorded with an HP 54510A digitizing oscilloscope which we interfaced to an IBM PC enabling us to digitally store the temporal trace data. Figure 10 shows an example of 1.532μm pumped 1.645μm Er:YAG laser results. Pumping was done with a QE7 KIGRE Er:glass laser rod having an active area of 3mm diameter surrounded by a 0.5mm thick UV absorbing cladding material, thus making up a 4mm diameter total. The 1.532μm output beam had relatively poor mode quality judging from the unfocused burn spot, typically measuring 2mm across. The burn spot at the focal point of the 15cm bi-convex lens measured approximately 700μm across , but having a more regular round transverse profile. The Polaroid 667 film gave reasonably reliable beam profiles confirming the computed pump surface area of $A \approx 0.003 cm^2$.

Comparing the laser onset delay (LOD) from lasing traces such as those of Figure 10 for different Er concentrations but with similar energy inputs, we noted that LOD decreased with increasing Er concentration (for the same 1cm crystal length).

Furthermore, for a given Er concentration in YAG, the LOD increased as the pump energy decreased, which is as expected since a longer time is required to absorb sufficient pump energy to reach threshold.

The 1.645μm energy measurements were carried out using an experimental arrangement similar to that of Figure 9. The actual 1.645μm energy detected by the RJ7200 calorimeter was properly calibrated by the previously determined attenuation factors of the microscope slide at 45° incidence, and the notch filter. Both the Scientech 365 and the RJ7200 calorimeters were calibrated with the aid of an energy meter which had been carefully calibrated against standard sources. The residual 1.532μm light that made it through to the RJ7200 calorimeter was subtracted from the readings. Because of the inherently high rejection ratio of our arrangement, this 1.532μm background energy turned out to be ≤ 10% of the 1.645μm energy. The energy measurements combined with temporal lasing traces enabled us to obtain input absorbed energy versus output data for the Er:YAG lasers.

The threshold energies and slope efficiencies were determined from lasing traces such as those in Figure 10 and the temporally resolved energy absorbed. Output versus input results for several Er:YAG crystals are shown in Figures 11. The Er:YAG crystals studied are listed in Table 1. The results for our measured laser thresholds were in good agreement with the

theoretical modeling which excluded upconversion losses and implied that upconversion should be small for these lasers.

TABLE 1. 1.532μm PUMPED1.645μm Er:YAG LASER PERFORMANCE

| Er:YAG Crystal | Er [%] | Length [cm] | αL | threshold [mJ] | | slope efficiency [%] |
|---|---|---|---|---|---|---|
| | | | | experiment | calculated | |
| 1 | 0.5 | 1 | 0.5 | 10 | 7 | 40 |
| 2 | 1 | 1 | 1 | 11 | 9 | 16 |
| 3 | 2 | 1 | 2 | 12 | 14 | 4.4 |
| 4 | 4 | 0.25 | 1 | 11 | 9 | 2.3 |

## THEORETICAL ANALYSIS

### Modified Franz-Nodvik (MFN) solution to the radiation transport equation

The solution of the radiation transport equation has been done by several authors[20,21,22]. The review of some of these approaches has been done by Siegman[23]. Avizonis and Grotbeck[22] presented an analytical solution to the radiation transport equation with the inclusion of passive losses. In all of these cases, the underlying method of solving the radiation transport equation involves the compression of one of the (time or space) variables. The standard approach[20,21,23] involves the compression of the spatial variable (along the propagation direction). The solution of the space compressed system as per Siegman[23] , modified to include Stark energy level structure (see

Figure 12), proceeds as follows: The two coupled differential equations describing energy the propagation of an energy pulse (or wave) through an active two level medium are:

$$\frac{dI}{dz} = -\sigma I(f_1 N_L - f_2 N_u) \qquad (1)$$

$$\frac{dN_u}{dt} = \frac{\sigma I}{h\nu}(f_1 N_L - f_2 N_u) \qquad (2),$$

where $N_L$ , $N_u$ are the lower and the upper population densities respectively with the corresponding Boltzmann factors, $f_1$ and $f_2$. The above two level model assumes no decay from the excited state, $N_u$, thus, giving an upper efficiency limit of a pulse propagating through an absorbing medium.

Numerical Integration Model (NIM) solution of the radiation transport equations including upconversion effects

The dominant method of upconversion excitation in $Er^{+3}$ crystals is the ion-pair cooperative non-radiative excitation which is the major excitation mechanism for the 3μm Er lasers[14]. The relevant rate equations for the 1.5μm pumped 1.6μm Er laser (Figure 12), modified to include Stark energy level structure, are:

$$\frac{dN_1}{dt} = -\sigma S(f_1 N_1 - f_2 N_2) + \frac{N_2}{\tau_2} + \frac{N_3}{\tau_{31}} + \beta N_2^2 \qquad (3)$$

$$\frac{dN_2}{dt} = \sigma S(f_1 N_1 - f_2 N_2) - \frac{N_2}{\tau_2} + \frac{N_3}{\tau_{32}} - 2\beta N_2^2 \qquad (4)$$

$$\frac{dN_3}{dt} = -\frac{N_3}{\tau_3} + \beta N_2^2 \qquad (5)$$

where $\frac{1}{\tau_3} = \frac{1}{\tau_{32}} + \frac{1}{\tau_{31}}$, $N_1$, $N_2$, and $N_3$ are the population densities of the $^4I_{15/2}$, $^4I_{13/2}$, and $^4I_{11/2}$ levels respectively. $\sigma$, S, and $\beta$ are the pump cross-section, the pump flux, and the ion-pair upconversion coefficient respectively. The pump flux is defined as $S = \frac{I_p}{h\nu_p}$ where $I_p$ is the pump intensity and $h\nu_p$ is the pump photon energy. In our numerical calculations we used the following values for the $Er^{3+}$ lifetimes: $\tau_2 \approx 7$ms, $\tau_{31} \approx 0.1$ms , and $\tau_{32} \approx 10$ms. The values for $\beta$ were obtained form the empirically determined variation of the upconversion coefficient in Er:YAG as function of Er concentration[25]. Equations (3-5) were numerically solved using the Runge-Kutta method.

The population inversion is defined as (with reference to Figure 12) as

$$\Delta N_0 = f_3 N_2 - f_4 N_1 = (f_3 + f_4) N_2 - f_4 N_t \qquad (6)$$

($f_3$ and $f_4$ are the Boltzmann factors for the laser levels). The threshold gain coefficient, $\gamma_{th}$, is determined as follows:

$$R_1 R_2 e^{2\sigma_L \Delta N L - \delta} = 1 \qquad (7)$$

$$\sigma_L \Delta N_{th} = \gamma_{th} = \frac{1}{2L}\left[\delta + \ln\left(\frac{1}{R_1 R_2}\right)\right] \approx \frac{1}{2L}(\delta + T) \qquad (8)$$

where $\delta$ is the round trip loss. The above expressions are valid for small output coupling, T. Using (6) and (8), we calculated the theoretical thresholds listed in Table 1.

## DISCUSSION

Since the upper manifold lifetime of the absorbing (lasing medium:Er:YAG) was long compared to the pump pulse [$\tau(^4I_{13/2})$ = 7ms][18], and at low Er doping concentrations upconversion and other parasitic energy transfer losses were negligible, the MFN model showed good agreement with the experimental bleaching data (Figure 5). There we plotted

experimental and theoretical (dashed curves) absorption coefficient as a function of input energy. The NIM model was in slightly better agreement with the 2%Er:YAG experimental bleaching results, although there was not a significant deviation from the ideal MFN model. These results indicate that upconversion losses do not significantly affect the population inversion densities in our lasers.

The upconversion fluorescence results of Figure 8 showed that regardless of the lifetime of the level from where fluorescence originates, the evolution of the fluorescence was delayed (peaks) by $\geq$ 600μs with respect to the pump pulse onset. This supports our results which indicate that the laser thresholds, typically achieved within a ≈200μs delay with respect to the beginning of the pump pulse, would be minimally increased by upconversion losses.

From the temporally resolved energy absorbed plots we obtained the pump energy thresholds and the energy absorbed during lasing using the temporal lasing traces such those of Figure 10. The threshold energies and the energies absorbed during lasing were subsequently combined with the measured 1.645μm output energy for known 1.532μm inputs, allowing us to plot the input versus output data shown in Figures 11. In our calculations we used the previously determined[28] stimulated emission cross-section for Er:YAG at 1.645μm ($\sigma_{1.645\mu m} \approx 1.9 \times 10\text{-}20 cm^2$ , also confirmed by our absorption measurements), with $\delta$=0.05 and T=0.05. The additional loss

term, $\delta \approx 0.05$, was determined from the estimated Fresnel losses in our resonator. Using this data we tabulated the experimentally determined and theoretically estimated thresholds, and the experimentally determined slope efficiencies for the Er:YAG lasers (see Table 1).

Table1. 1.532μm pumped 1.645μm Er:YAG laser performance.

| Er:YAG Crystal | Er [%] | Length [cm] | αL | threshold [mJ] | | slope efficiency [%] |
|---|---|---|---|---|---|---|
| | | | | experiment | calculated | |
| 1 | 0.5 | 1 | 0.5 | 10 | 7 | 40 |
| 2 | 1 | 1 | 1 | 11 | 9 | 16 |
| 3 | 2 | 1 | 2 | 12 | 14 | 4.4 |
| 4 | 4 | 0.25 | 1 | 11 | 9 | 2.3 |

From Table 1, we note the good agreement between our experimental measurements of laser thresholds and the theoretical estimates which did not include upconversion losses. This shows that Er(0.5-4%):YAG lasers should be operable with only small degradation due to upconversion. Additional evidence is shown in Figure 5. The good agreement between our theoretically estimated (NIM and MFN models) and experimentally determined absorption coefficients of the Er(0.5-2%):YAG samples at pumping levels exceeding those utilized in our laser experiments shows that low concentration Er:YAG lasers without deleterious effects of upconversion are feasible. The above results are consistent with the work of references [19] and [20] which show that pair upconversion losses from the

$^4I_{13/2}$ level in $Er^{3+}$(<4%):crystals (such as YLF and YAG) are small and should not appreciably inhibit laser action.

The data in the last column of Table 1, which lists the slope efficiency of our Er:YAG lasers, shows a decreasing efficiency with increasing Er concentration. For the 0.5%Er:YAG the measured slope efficiency of ≈40% is in good agreement with the theoretically deduced value of 45% where we assumed, as before, $\delta=T\approx0.05$. This is consistent with the theoretical calcuations showing excellent agreement between theoretical and experimental thresholds (see Table 1). The observed progressively decreasing slope efficiencies of samples 2-4 is currently still under investigation.

The effect which could reduce our slope efficiencies for samples 2-4 (see Table 1), and which we believe responsible for the results obtained, is increasingly poorer overlap of the pump and laser beams with increasing Er concentration. A major contributing factor is that we are pumping longitudinally with an approximately Gaussian radial (transverse) intensity distribution. Thus, only the central portion of our Gaussian beam is effective in pumping the Er:YAG samples. This effect (which is most severe in quasi-three level lasers) becomes stronger for the more concentrated samples.

A closely related effect was observed in our work on saturable absorber Q-switches. When the saturable absorber Q-switch is inserted in the laser cavity, the diameter of the laser

beam is reduced by approximately a factor of two[29]. This effect could result in a drastic reduction of pump and laser mode overlap; however, further work is required and is in progress in order to clarify the Er(1-4%):YAG laser results.

## CONCLUSIONS

The laser dynamics of 1.532μm pumped 1.645μm Er:YAG at 300K were studied and analyzed. Good agreement between the experimentally determined thresholds for Er(0.5-4%):YAG and theoretical estimates (which did not include upconversion losses) showed the feasibility of efficient laser operation. This was confirmed by the demonstration of a 40% slope efficiency Er(0.5%):YAG laser in a non-optimized laser cavity, in agreement with theoretical estimates.

## ACKNOWLEDGEMENT

The authors thank Mr. John D. Myers, president of Kigre Inc., for the generous gift of the Er, Yb:phosphate glass laser rods used in this work.

## REFERENCES


1. Z. J. Kiss and R. C. Duncan Jr. ,"Optical Maser Action in $CaWO_4:Er^{+3}$" Proc. IRE **50**,1531 (1962)

2. S. A. Pollack, "Stimulated Emission in $CaF_2:Er^{+3}$", Proc. IEEE **51**,1793-1794 (1963)

3. W. F. Krupke and J. B. Gruber, "Energy Levels of $Er^{+3}$ in $LaF_3$ and coherent emission at 1.61μ", J.Chem. Phys.**41**(5),1225-1232 (1964)

4. L. F. Johnson, J. E. Geusic and L. G. VanUitert, "Coherent Oscillations from $Tm^{+3}$, $Ho^{+3}$, $Yb^{+3}$, and $Er^{+3}$, ions in Yttrium Aluminum Garnet", Appl.Phys.Lett. **7**(5),127-129(1965)

5. K. O. White and S. A. Schleusener, "Coincidence of Er:YAG laser emission with methane absorption at 1645.1nm", Appl.Phys.Lett. **21**,419-420 (1972)

6. G. Huber, E. W. Duczynski, and K. Petermann, "Laser pumping of Ho-, Tm-, Er-doped Garnet lasers at room temperature", IEEE J.Quant. El tron. **24**(6),920-923 (1988)

7. H. Stange, K. Petermann, G. Huber, and E. W. Duczynski, "Continuous wave 1.6μ laser action in Er-doped garnets at room temperature", Appl.Phys.B **49**,269-273 (1989)

8. K. Spariosu and M. Birnbaum, "Room temperature 1.645 micron Er:YAG lasers", OSA Proc. on Advanced Solid-State Lasers, Feb.17-19, Santa Fe, New Mexico, 127-130 (1992).

9. G. M. Zverev, V. M. Garmash, A. M. Onishchenko, V. A. Pashkov, A. A. Semenov, Yu. M. Kolbatskov, and A. I. Smirnov, "Induced emission by trivalent erbium ions in crystals of yttrium-aluminum garnet", J.Appl.Spectrosc.(USSR), **21**,1467-1469(1974).

10. F. Auzel, "Materials and devices using double-pumped phosphors with energy transfer", Proc. IEEE, **61**(6), 758-786 (1973).

11. L. Riseberg and M. Weber, "Relaxation phenomena in rare-earth luminescence", in "Progress in optics XIV", ed. E.Wolf (North Holland, 1976), 92-159.

12. J. Wright, "Up-conversion and excited state energy transfer in rare-earth doped materials", in "Topics in Applied Physics," ed. F.K. Fong, Vol. 16 (Springer-Verlag, 1976), 239-295.

13. S. Pollack, D. Chang, and N. Moise, "Upconversion-pumped infrared erbium laser", J.Appl.Phys. **60**(12), 4077-4086 (1986).

14. S. Pollack and D. Chang, "Ion-pair upconversion pumped laser emission in $Er^{3+}$ ions in YAG, YLF, $SrF_2$, and $CaF_2$ crystals", J.Appl.Phys. **64**(6), 2885-2893 (1988).

15. P. Xie and S. Rand, "Continuous-wave, pair-pumped laser", Opt. Lett. **15**(15), 848-850 (1990).

16. P. Xie and S. Rand, "Continuous-wave, trio upconversion laser", Appl.Phys.Lett. **57**(12), 1182-1184 (1990).

17. S. Pollack, D. Chang, and M. Birnbaum "Threefold upconversion pumped laser at 0.85, 1.23, and 1.73μm in Er:YLF *pumped with a* 1.53μm Er:glass laser", Appl.Phys.Lett. **54**(10), 869-871 (1989).

18. S. Pollack, D. Chang, M. Birnbaum, and M. Kokta, "Upconversion-pumped 2.8-2.9μm lasing of $Er^{3+}$ ion in garnets", J.Appl.Phys. **70**(12), 7227-7239 (1991).

19. R. A. McFarlane, M. Robinson, S. A. Pollack, D. B. Chang, and H. Jenssen, "Visible and infrared laser operation by upconversion pumping of Erbium-doped fluorides", in Tunable Solid State Lasers, Vol. **5**, 1989, pp179-186.

20. V. I. Zhekov, T. M. Murina, A. M. Prokhorov, M. I. Studenikin, S. Georgescu, V. Lupei, and I. Ursu, "Cooperative process in

$Y_3Al_5O_{12}:Er^{3+}$ crystals", Sov. J. Quantum Electron. **16**(2), 274-276, (1986).

21. V. P. Gapontsev, M. E. Zhabotinskii, A. A. Izyneev, V. B. Kravchenko, and Yu. P. Rudnitskii, "Effective 1.054-1.54μ stimulated emission conversion", JETP Lett. **18**,251-253 (1973).

22. L. M. Franz and J. S. Nodvik, "Theory of pulse propagation in a laser amplifier", J.Appl. Phys. **34**(8), 2346(1963).

23. R. Bellman, G. Birnbaum, and W. G. Wagner, "Transmission of monochromatic radiation in a two-level material", J.Appl.Phys.**34**(4), 780(1963)

24. P. V. Avizonis and R. L. Grotbeck, "Experimental and theoretical ruby laser amplifier dynamics", J.Appl.Phys. **37**(2), 687(1966).

25. A. Siegman, "Lasers", University Science Books (Mill Valley, CA, 1986), pp 363-372.

26. S. Georgescu, V. Lupei, A. Lupei, V. I. Zhekov, T. M. Murina, and M. I. Studenikin, "Concentration effects on the upconversion from the $^4I_{13/2}$ level of $Er^{+3}$ in YAG", Opt.Comm.**81**(3,4)186(1991).

27. D. K. Killinger, "Er:YAG laser crystal characterization", Quarterly technical report, Solid-state research, Lincoln Laboratory, M.I.T., Lexington, Massachusetts, pg 9 (Nov., 1985).

28. R.D.Stultz, M.B.Camargo, S.T.Montgomery, M.Birnbaum, and K.Spariosu, "$U^{4+}$:$SrF_2$ efficient saturable absorber Q-switch for the 1.54μm Er:glass laser", Accepted for publication and scheduled to appear in Feb., 1994 issue of Applied Physics Letters.

## List of Figures

Figure 5. Absorption saturation in 1cm thick 0.5,1,2% Er:YAG crystals. The dashed curves represent the MFN model and the solid curves represent the NIM model.

Figure 6. Incident and transmitted 1.532μm spiking pulses, and the corresponding integrated 1.532μm incident and transmitted energy pulses (spiking signals not to scale).

Figure 7. Experimental arrangement for upconversion fluorescence measurements.

Figure 8. 1.532μm pumped 980nm upconversion fluorescence in Er:YAG (4%,1%,2% lowest-highest). The rectangle represents the 1.532μm pump pulse. The small peaks at the beginning are due to scattered flashlamp radiation and the large delayed peaks are those due to upconversion fluorescence.

Figure 9. Experimental arrangement for measuring the Er:YAG laser characteristics.

Figure 10. 1.645μm laser output (top trace) with the corresponding 1.532μm pump (lower trace) for the 1%Er:YAG laser.

Figure 11. Er:YAG laser energy output performance.

Figure 12. $Er^{3+}$:YAG energy level diagram (300K) showing the 1.532μm pumped 1.645μm laser transition and the appropriate Boltzmann factors.

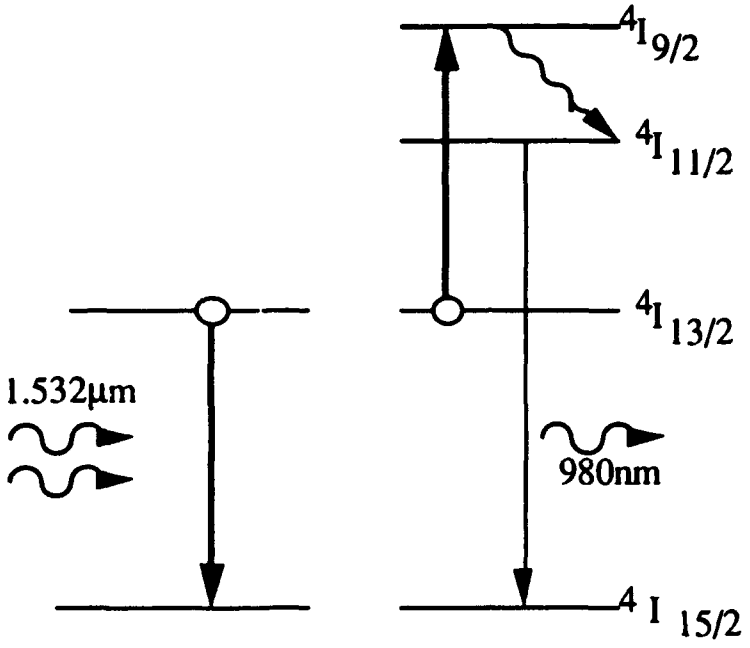


Figure 1. Energy level diagram for $Er^{3+}$ showing the ion pair upconversion effect and the resulting upconversion fluorescence.

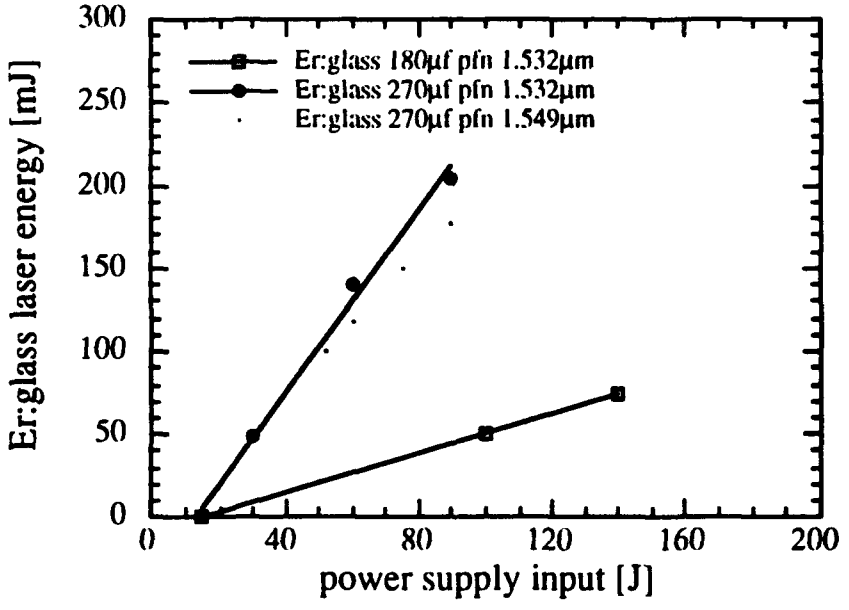


Figure 2. QE7 Er:glass laser performance at 1.532μm

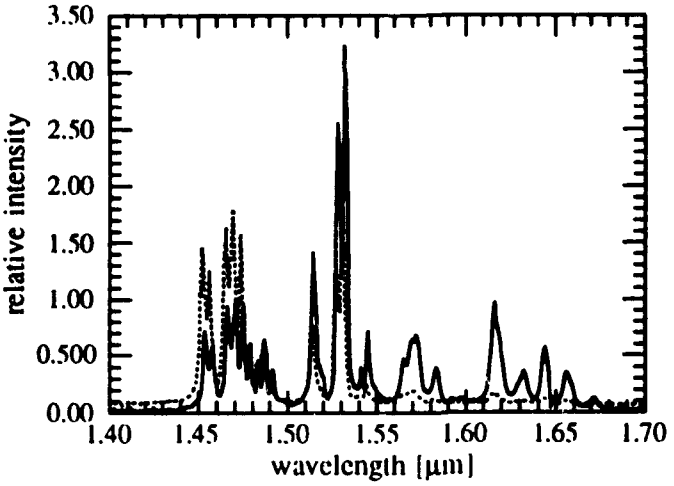


Figure 3. 0.5%Er:YAG absorption (dashed curved) and photoluminescence (solid curve)

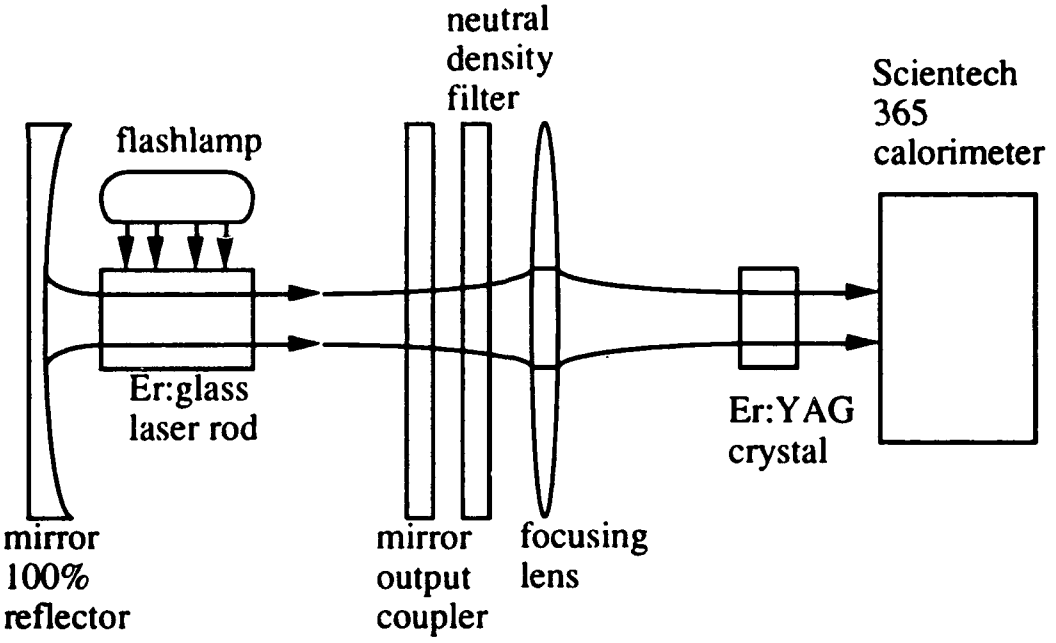


Figure 4. Experimental arrangement for absorption (and bleaching) measurements

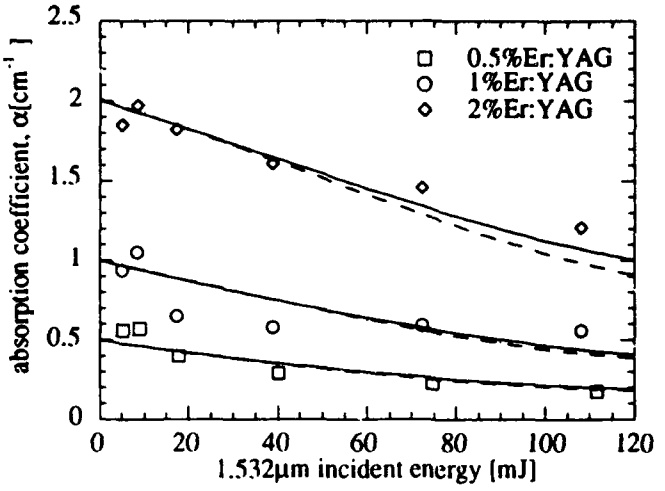


Figure 5. Absorption saturation in 1cm thick 0.5, 1.2% Er:YAG crystals; dashed curves:MFN model; solid curves:NIM model

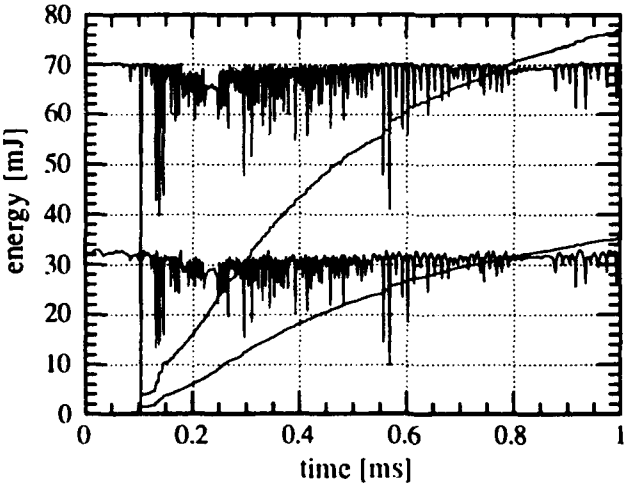


Figure 6. 4%0.25cm Er:YAG spiking and corresponding integrated 1.532μm incident and transmitted energy (spiking signals not to scale)

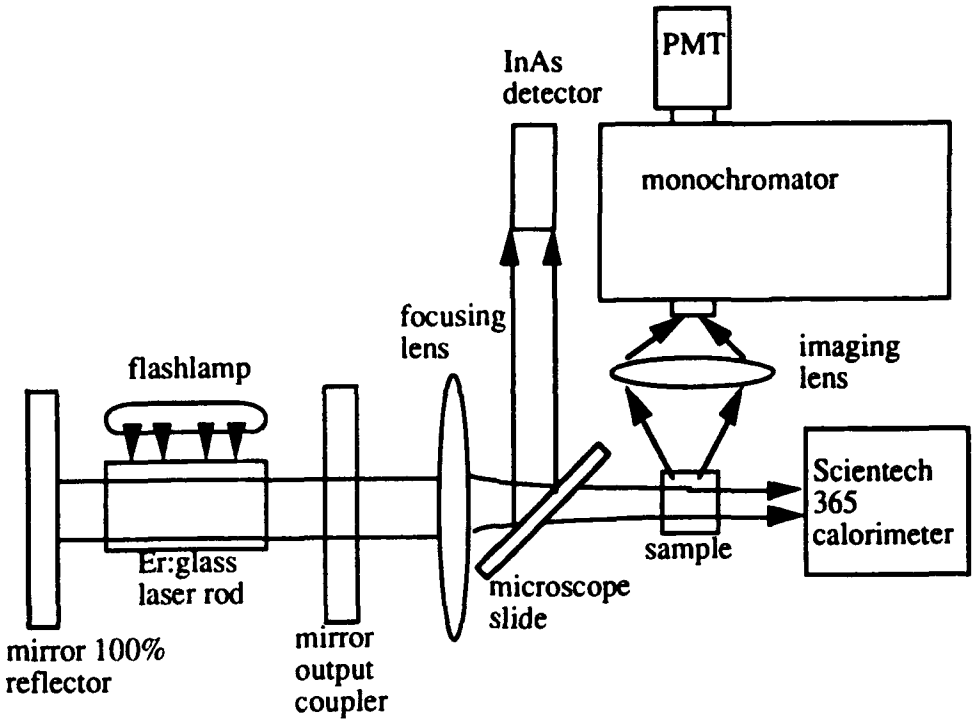


Figure 7. Experimental arrangement for upconversion fluorescence measurements.

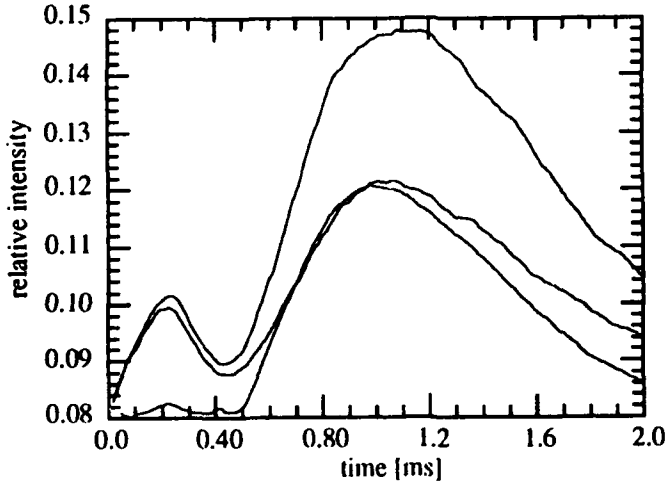


Figure 8. 1.532μm pumped 980nm upconversion fluorescence in Er:YAG (4%,1%,2% lowest-highest); rectangle depicts the temporally relative position of the pump pulse

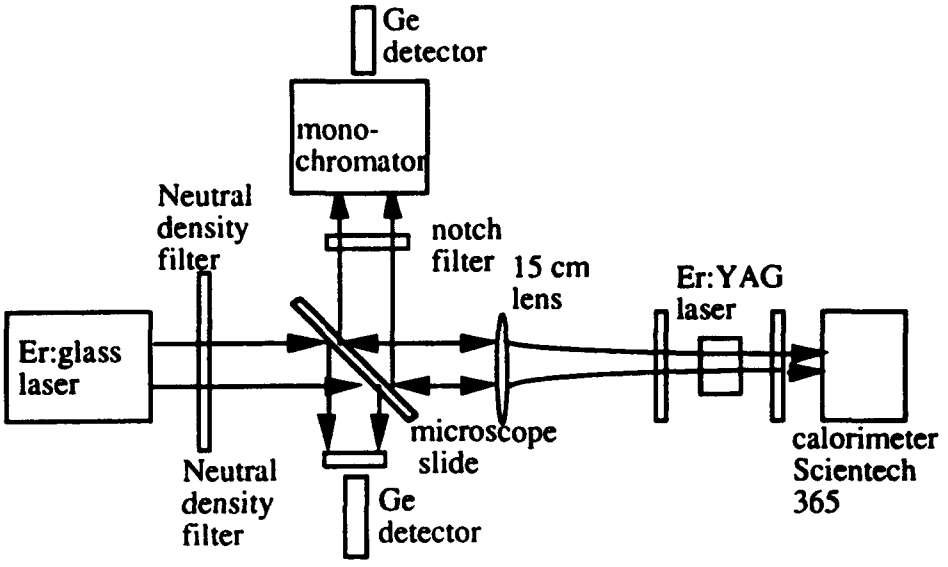


Figure 9. Experimental arrangement for measuring the Er:YAG laser charactersistics.

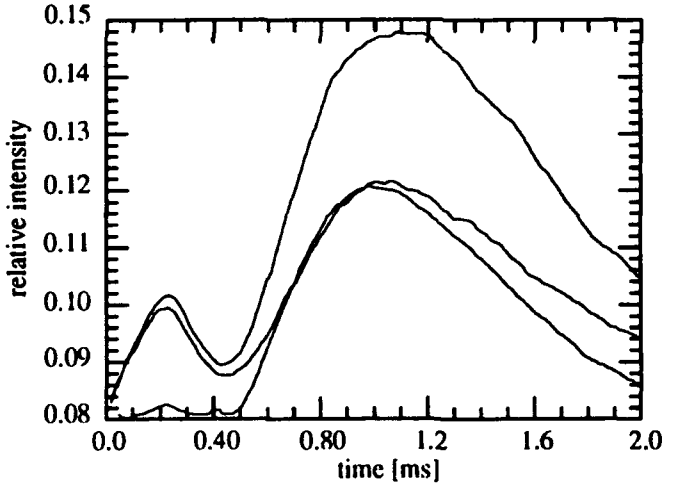


Figure 10. 1%Er:YAG 1.645μm laser output (top trace) lower trace:1.532μm pump (120mJ)

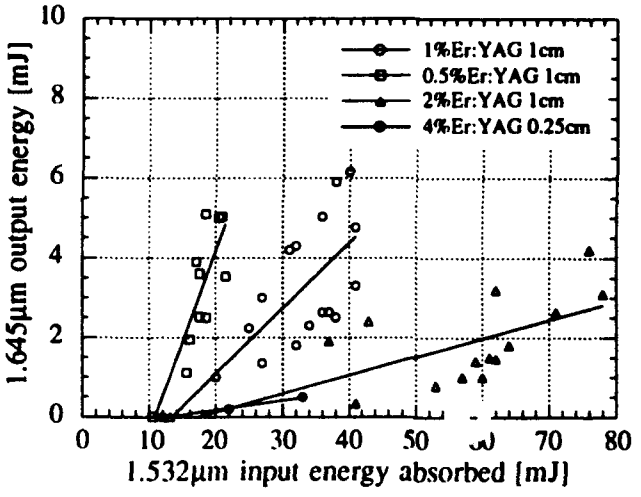


Figure 11. Er:YAG laser energy output performance

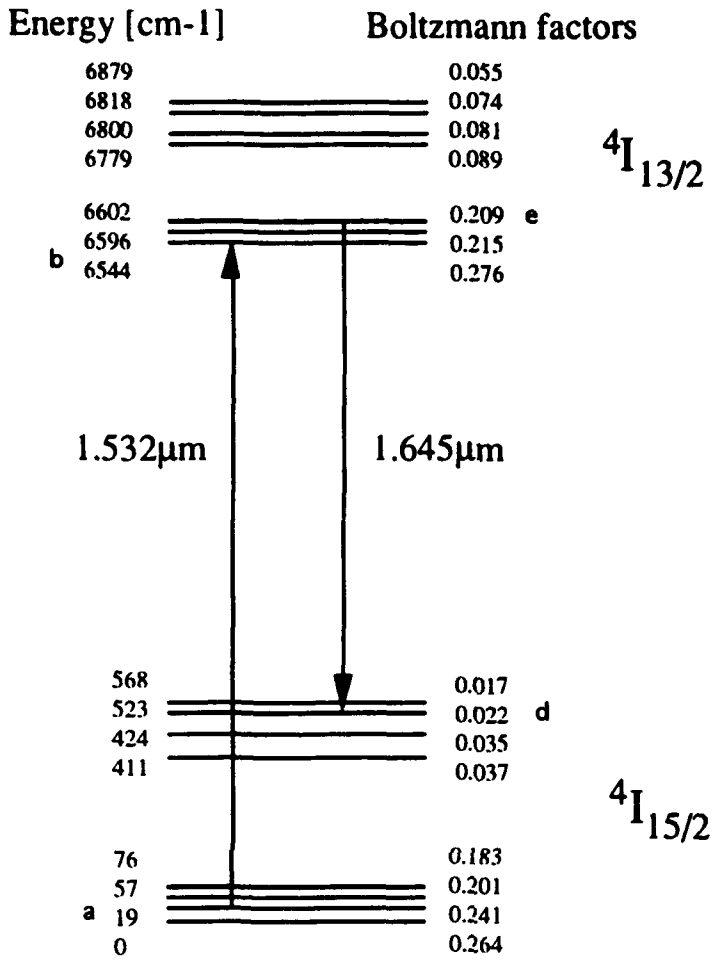


Figure 12. $Er^{3+}$:YAG energy level diagram (300K) showing the 1.532μm pumped 1.645μm laser transition and the appropriate Boltzmann factors.

# 1.643μ $Er^{3+}:Y_3Sc_2Ga_3O_{12}$ (Er:YSGG) laser at 300K

by:

Kalin Spariosu and Milton Bimbaum
Center for Laser Studies
University if Southern California
DRB B17, University Park
Los Angeles, CA 90089-1112

and:

Milan Kokta,
Union Carbide Corp.
Washougal, Washington 98671

## Abstract

The first $^4I_{13/2}$-$^4I_{15/2}$ laser transition at 1.643μ in $Er^{3+}$:$Y_3Sc_2Ga_3O_{12}$ (Er:YSGG) at 300K is reported. An Er:glass laser (1.532μ) was used in an end pumping arrangement to obtain laser output from a 1cm long 0.7%Er(3%Yb,1%Cr):YSGG crystal in an external cavity. The Er:YSGG laser exhibited a 20mJ threshold and a 8% slope efficiency.

## Introduction

The first $^4I_{13/2}$-$^4I_{15/2}$ laser action near 1.6μ was demonstrated in Er:$CaWO_4$[1] followed by reported laser action in Er:$CaF_2$[2], and in Er:$LaF_3$[3], all near 1.6μ. All the above reports utilized flash lamp pumping at 77K. The first 1.645μ $^4I_{13/2}$-$^4I_{15/2}$ laser action in Er:YAG was achieved by Johnson et al[4] at 77K and later at room temperature as reported by White and Schleusener[5] , again using flash lamp excitation in both cases. More recently, CW oscillation at 1.645μ in Er:YAG was achieved using a Kr ion laser at 0.647μ in an end pumping arrangement[6,7] We reported on 1.532μ pumped 1.645μ Er:YAG lasers at 300K in a standard outside cavity pumping arrangement using an Er:glass laser as the pump source in an end pumped configuration[8] Here, we report on the first 1.643μ laser action in the $^4I_{13/2}$-$^4I_{15/2}$ transition in Er:YSGG.

## Experimental Results

Absorption measurements of our uncoated 1cm thick 0.7%Er(3%Yb,1%Cr):YSGG crystal (with parallel and polished faces) were obtained using a Varian CARY model 2415 spectro-photometer (see Figure 1). The small signal absorption coefficient of 0.7%Er:YSGG at the 1.532μm Er:glass pump laser wavelength was determined to be $\alpha = 0.84\ cm^{-1}$. The determination of α was carried out after first calibrating out the surface reflection (Fresnel) losses

(≈12%) but including the rest of the base line background in our calculation (see Figure 1). The small signal absorption, $\alpha L=0.84$, was confirmed using the 1.532μm Er:glass laser[9] at low output levels.

We repeated the absorption spectra measurements several times using the CARY and consistently obtained roughly the same background base line. We did not observe a wavelength dependent base line variation (as would be indicative of $Cr^{4+}$ absorption), and, therefore, concluded that the origin of this residual base-line absorption could be attributed to poor crystal quality. At 300K the individual Stark lines were not resolved (as would be possible at cryogenic temperatures).

Measurements of the induced transparency (bleaching) in our Er:YSGG crystal were obtained using the 1.532μm Er:glass laser as the pump . The bleaching results are shown in Figure 2 (the theoretical curve was obtained using the theoretical analysis outlined in a following section of the paper). A photoluminescence experiment was carried out on the Er:YSGG crystal, and the results are shown in Figure 3. From the identified fluorescence peak in Figure 3, and from the Er:YSGG energy level diagram[10] of Figure 4 we identified the 1.643μ lasing transition to be $^4I_{13/2}$:z3(6596cm$^{-1}$)-$^4I_{15/2}$:y8(509cm$^{-1}$).

The laser pumped lasing experimental arrangement is shown in Figure 5. The Er:glass laser pump laser operated in a single shot mode at 1.532μ, utilizing a flat-flat resonator. A typical free running spiking Er:glass laser output was approximately 1.5ms in duration.

In order to separate the 1.643μ Er:YSGG output from the stronger Er:glass laser output at 1.532μ, a notch filter (1.532μ to 1.643μ rejection ratio of 60 to 1) was used. The 1.643μ Er:YSGG laser light was sampled out of mirror M1, counter-propagating with respect to the 1.532μ Er:glass pump because M1 was the output coupler (T≈5%) at 1.643μ (see Figure 5). Furthermore, the small reflection (R≈10%) at 1.532μ from M1 provided for a higher 1.643μ to 1.532μ rejection ratio than would be available with ≈50% transmission of mirror M2 at 1.532μ in a co-propagating signal detection mode ($R_{1.643\mu m}$>99.9% for M2). The measurement of the Er:YSGG laser output wavelength was carried out using a Jarrell-Ash 0.25m monochromator. Laser action was obtained at 300K with a 0.7%Er(3%Yb,1%Cr):YSGG crystal 1cm long with ends polished flat, parallel and uncoated.

The spiking 1.643μ output of the 0.7% Er:YSGG laser is shown in the top trace of Figure 6, where the bottom trace shows the corresponding time coincident 1.532μ Er:glass pump. The signals were detected using Ge detectors and a dual beam HP 54510A digitizing oscilloscope. Typical duration of the free running spiking Er:glass output was 1.5ms. The 1.643μ laser action persisted for the duration of the 1.532μ pump pulse (after the laser onset delay). The 1.643μ output was shown to have a pulse to pulse correspondence with the pump (similar to the results found in Er:YAG lasers[8]), but with a slight delay.

The input versus output energy data is presented in Figure 7. We define the differential energy absorbed as the 1.532μ energy

absorbed during 1.643μ lasing, plus the measured 1.532μ energy absorbed required to reach threshold. The absorbed energy was determined using two calorimeters as shown in Figure 5. Several runs were made yielding a measured threshold of about 20mJ, and a slope efficiency of 8%. The calorimeters used were: Scientech 365 and the Laser Precision RJ7200. The Er:YSGG laser cavity was 5 cm long with flat-flat mirrors.

## Theoretical Analysis

The pulse propagation through an active (absorbing or amplifying) medium involves the solution of the radiation transport equation as presented by several authors[11-14]. The solution generally involves the compression of either the space or the time variable. Following the method of Siegman[14], we solved the following coupled equations:

$$\frac{d\Delta N(t)}{dt} = -\frac{2}{h\nu_p}\left[I_{in}(t)\left(e^{\sigma\Delta N(t)}-1\right)\right] \qquad (1)$$

$$U_{out}(t) = \int_{t_0}^{t} I_{out}(t)dt = U_{sat}\ln\left[\frac{\left(e^{\sigma\Delta N_0}-1\right)}{\left(e^{\sigma\Delta N(t)}-1\right)}\right] \qquad (2),$$

where $\Delta N$ is the spatially integrated localized population difference[14] ( units: [$cm^{-2}$]), $\sigma$ is the effective absorption cross-section, $\sigma_{eff}= 9.2x10^{-21}cm^2$, $h\nu_p$ is the pump photon energy, and $U_{sat}$ is the saturation fluence defined as $U_{sat}=\frac{h\nu}{\sigma}$ . The method of solution then involves the propagation of successive pulselets through the spatially segmented medium updating the level populations after each pulselet has gone through. The calculation was carried out numerically and the bleaching results are shown in Figure 2. As can be noted from Figure 2, there is close agreement between theory and experiment for a pumped volume of $0.005cm^3$, corresponding to the pump radius, $a\approx0.04cm$.

Threshold energy was evaluated as follows: Since the 1.643μm laser action occurs between the Stark levels y3 and z8, we can write the threshold condition as

$$N_{y3}-N_{z8}=\Delta N_{th} \qquad (3)$$

where the Stark levels are defined in terms of the total manifold populations (y:$^4I_{13/2}$, z:$^4I_{15/2}$) as

$$N_{y3}=\frac{f_{y3}}{Z_y}N_y \ , \ N_{z8}=\frac{f_{z8}}{Z_z}N_z \qquad (4)$$

$f_{y3}$, and $f_{z8}$ are the appropriate Boltzmann factors and the partition functions are:

$$Z_{y,z}=\sum_{i=1}^{(7,8)} e^{-\frac{\Delta E_i}{kT}} \qquad (5)$$

Taking into account Stark level structure and knowing that only a fraction of the absorbed photons contributes to the population inversion, we can write the equation for pump energy threshold as:

$$E_{th}=\frac{Vh\nu_p(\delta+T)}{2\sigma_L L(f_3+f_4)}+\frac{N_t f_4 Vh\nu_p}{(f_3+f_4)} \qquad (6)$$

where $N_t$ is the Er doping density, $f_3$ and $f_4$ are the Boltzmann factors of the laser levels, $\delta$ is the round trip cavity loss, T is the output coupling loss, $\sigma_L$ is the stimulated emission cross section, and $\nu_p$ is the pump laser frequency.

Given $T\approx 0.05$, $V=0.005cm^3$, and the experimentally determined value of $\sigma_L=1.7\times10^{-20}cm^2$ (from absorption spectra), we calculated the pump threshold energy ($\delta=0$, assumes only output coupler loss) to $\approx$9mJ. This is approximately a factor of two less than the experimentally determined threshold value of $\approx$20 mJ, indicative of the presence of additional losses. Our low slope efficiency (8%)

confirmed this observation. Enumerating factors contributing to inefficiency: imperfect pump/laser mode volume overlap, scattering losses, end reflection losses, etc. Clearly, additional work will be required to optimize this new laser.

## Conclusions

The first operation of the $^4I_{13/2}$-$^4I_{15/2}$ 1.643μm Er:YSGG laser at 300K is described. The 0.7% Er:YSGG laser had operated quasi-CW, with the 1.643μm laser action persisting for the duration of the 1.532μm pump pulse (after the onset delay).

## Acknowledgements

We thank Mr. John Meyers of the KIGRE Corp. for the gift of several KIGRE Er:phosphate glass laser rods used in these experiments.

## References


1. Z.J.Kiss and R.C.Duncan Jr. ,"Optical Maser Action in $CaWO_4:Er^{+3}$" Proc. IRE **50**,1531 (1962).
2. S.A.Pollack, "Stimulated Emission in $CaF_2:Er^{+3}$", Proc. IEEE **51**,1793-1794 (1963).
3. W.F.Krupke and J.B.Gruber, "Energy Levels of $Er^{+3}$ in $LaF_3$ and coherent emission at 1.61μ", J.Chem. Phys.**41**(5),1225-1232 (1964).
4. L.F.Johnson, J.E.Geusic and L.G.VanUitert, "Coherent Oscillations from $Tm^{+3}$, $Ho^{+3}$, $Yb^{+3}$, and $Er^{+3}$, ions in Yttrium Aluminum Garnet", Appl.Phys.Lett. **7**(5),127-129 (1965).
5. K.O.White and S.A.Schleusener, "Coincidence of Er:YAG laser emission with methane absorption at 1645.1nm", Appl.Phys.Lett. **21**,419-420 (1972).
6. G.Huber, E.W.Duczynski, and K.Petermann, "Laser pumping of Ho-, Tm-, Er-doped Garnet lasers at room temperature", IEEE J.Quant. Electron. **24**(6), 920-923 (1988).
7. H.Stange, K.Petermann, G.Huber, and E.W.Duczynski, "Continuous wave 1.6μ laser action in Er-doped garnets at room temperature", Appl.Phys.B **49**, 269-273 (1989).
8. K.Spariosu and M. Birnbaum, "Room temperature 1.645 micron Er:YAG lasers", OSA Proceedings on Advanced Solid-State Lasers, Feb.17-19, 1992, Santa Fe, New Mexico, p127-130.
9. E.Zharikov, N.N.Il'ichev, S.P.Kalitin, V.V.Laptev, A.A.Malyutin, V.V.Osiko, P.P.Pashinin, A.M.Prokhorov, Z.V.Saidov, V.A.Smirnov, A.F Umyskov, and I.A.Shcherbakov, "Spectral, luminescence, and lasing properties of a yttrium scandium gallium garnet crystal activated with chromium and erbium", Sov. J. Quantum Electron. **16**, 635-639 (1986).
10. Lee M. Frantz and John S. Nodvik, "Theory of pulse propagation in a laser amplifier", J.Appl. Phys. **34**(8), 2346-2349 (1963).
11. R.Bellman, G.Birnbaum, and W.G.Wagner, "Transmission of monochromatic radiation in a two-level material", J.Appl.Phys.**34**(4), 780-782 (1963).

12. P.V.Avizonis and R.L.Grotbeck, "Experimental and theoretical ruby laser amplifier dynamics", J.Appl.Phys. 37(2), 687-693 (1966).
13. A.Siegman, "Lasers", University Science Books (Mill Valley, CA, 1986),pg 363-372.

## Figure Captions

Figure 1. Absorption spectra of 0.7%Er(Yb,Cr):YSGG (theoretical curve was obtained using the numerical calculations outlined in the text).
Figure 2. Absorption saturation in 0.7%Er(Yb,Cr):YSGG (experimentaland theoretical).
Figure 3. Photoluminescence spectra for 0.7%Er(Yb,Cr):YSGG.
Figure 4. Er:YSGG energy level diagram at 300K.
Figure 5. Experimental arrangement for measuring the 0.7%Er(Yb,Cr):YSGG. laser performance.
Figure 6. 1.532μm (bottom trace) pumped 1.643μm laser action (top trace) (100μs per division).
Figure 7. 1.643μm 0.7%Er(Yb,Cr):YSGG laser output as a function of 1.532μm pump energy absorbed.

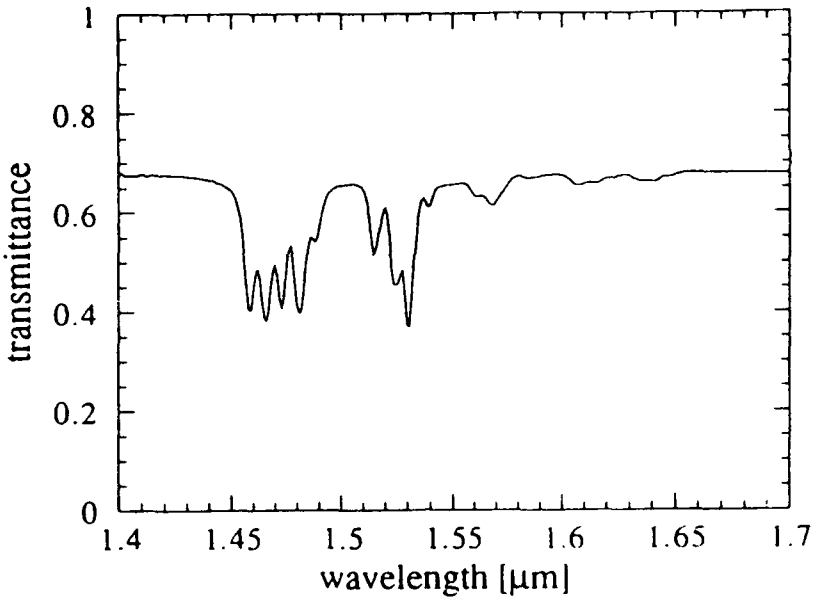


Figure 1: 0.7% Er:(Yb,Cr) YSGG absorption

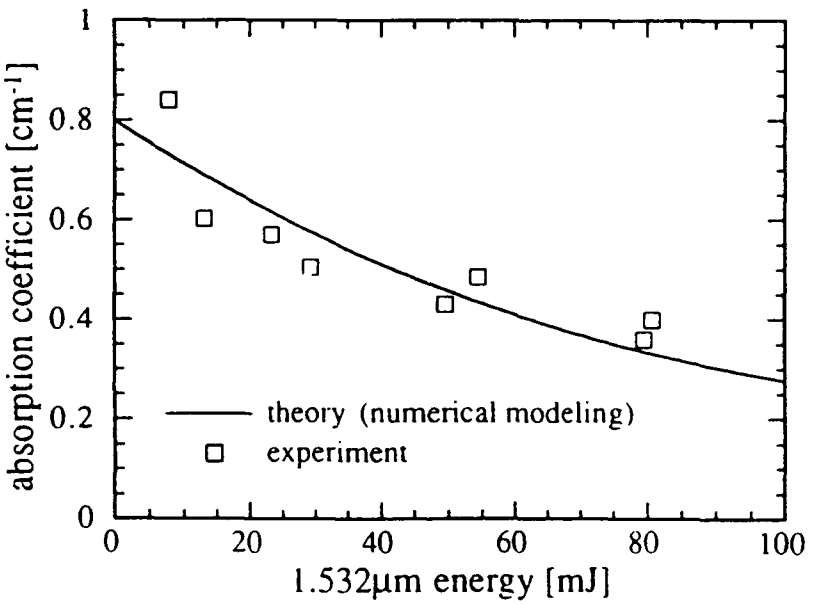


Figure 2: Absorption saturation in 0.7%Er(Yb, Cr):YSGG
(theoretical curve was obtained using the
numerical modeling outlined in the text)

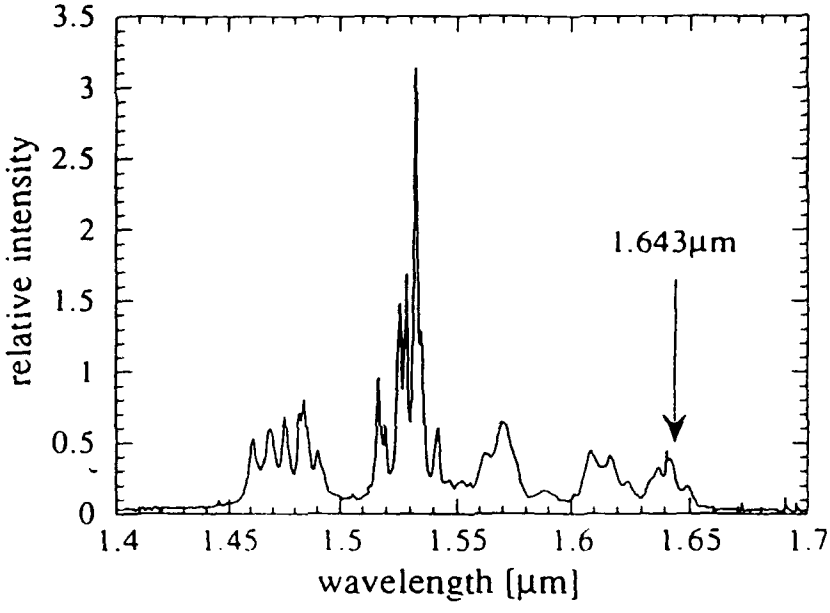


Figure 3: 0.7% Er:YSGG photoluminescence

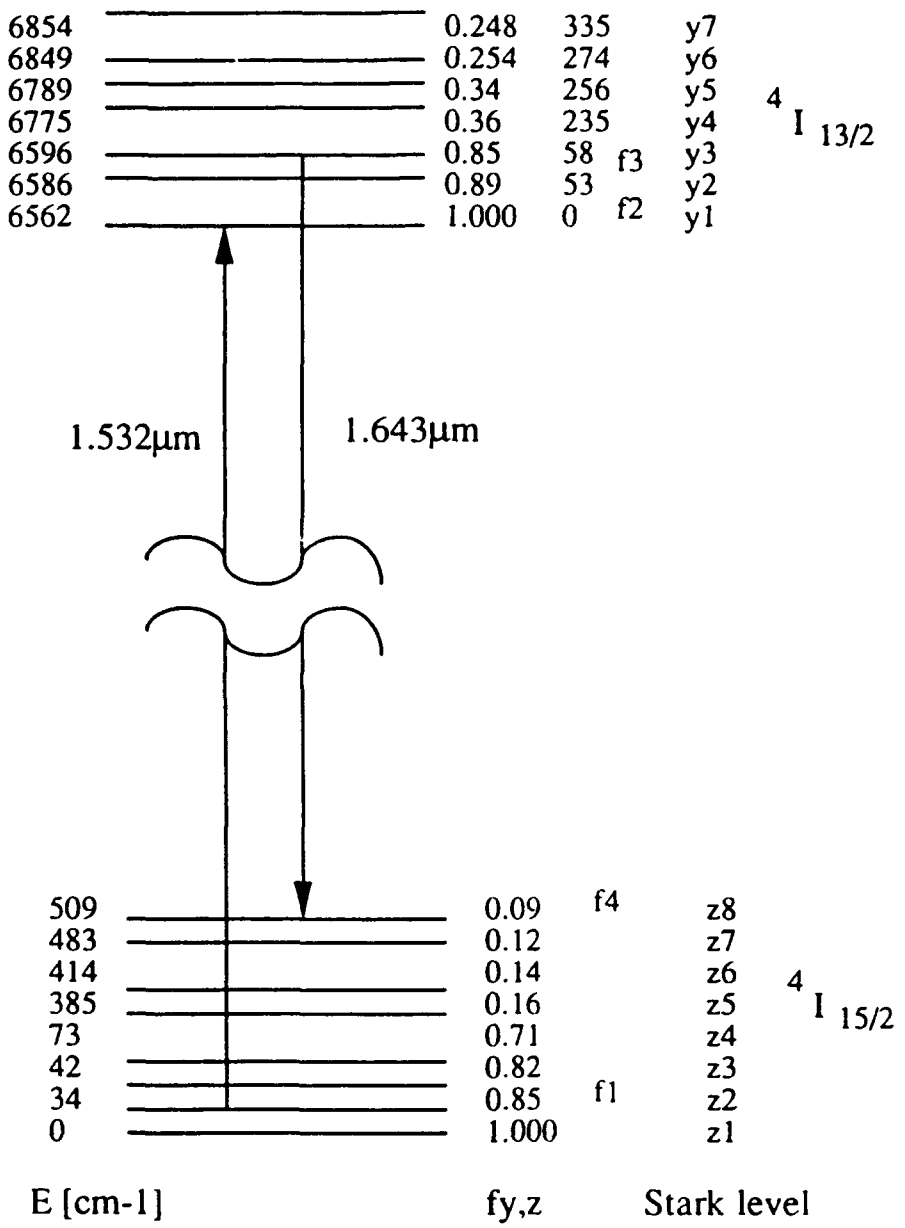


Figure 4. Stark energy level diagram for the ground and first excited states of Er:YSGG at 300K.

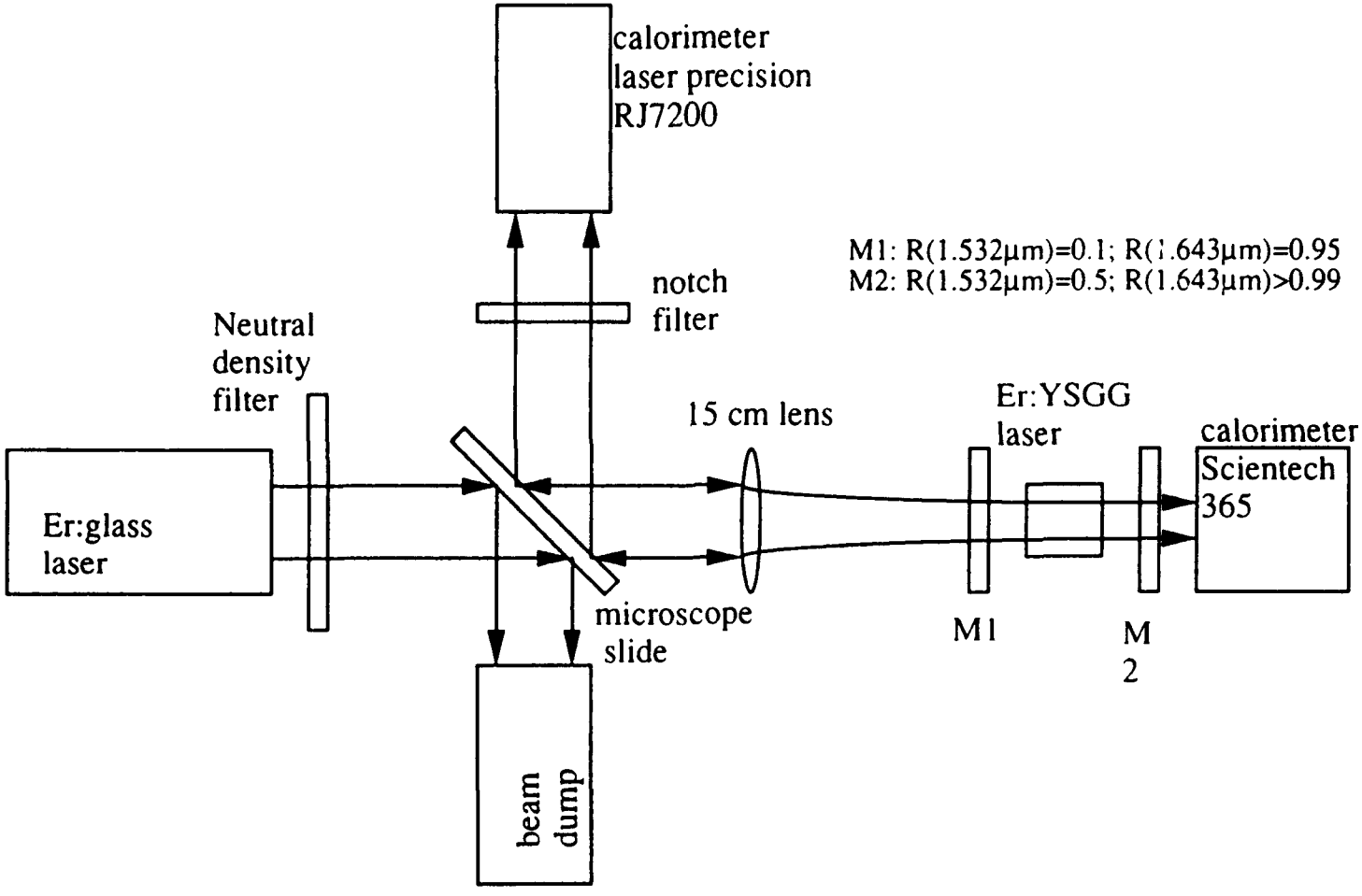


Figure 5. Experimental set-up for measuring the Er:YSGG laser performance

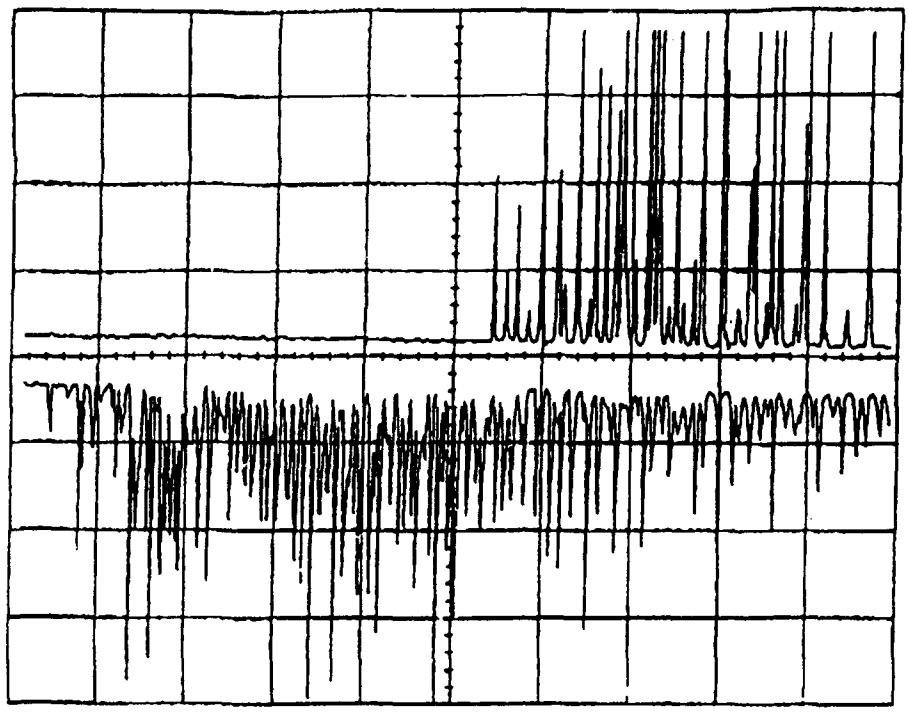

Figure 6. 1.532μm (bottom trace) pumped 1.643μm laser action (top trace) (100μs per division).

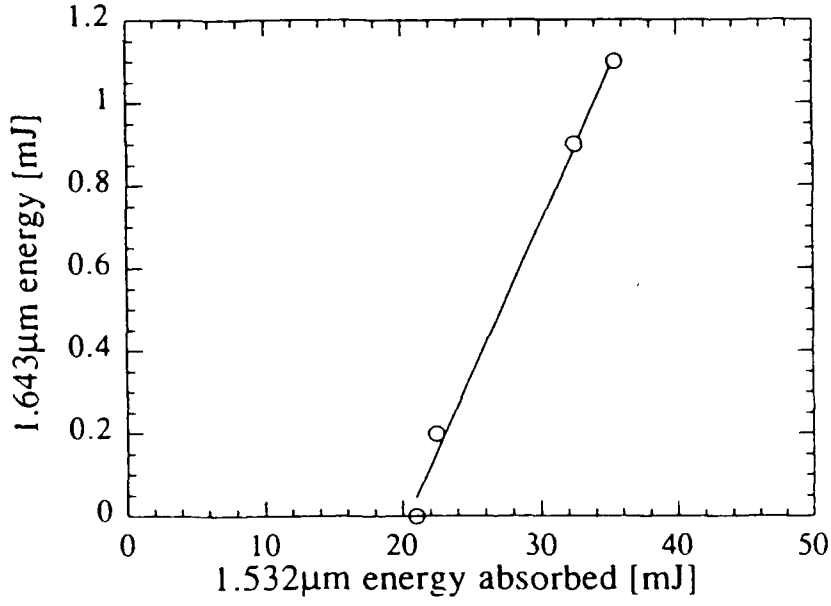


Figure 7: 0.7% Er:YSGG laser output